

THE UNIVERSITY OF NEW SOUTH WALES
SCHOOL OF PHYSICS
Higher Year Laboratory

ACOUSTO- OPTICS

AO

FOLDER CONTENTS

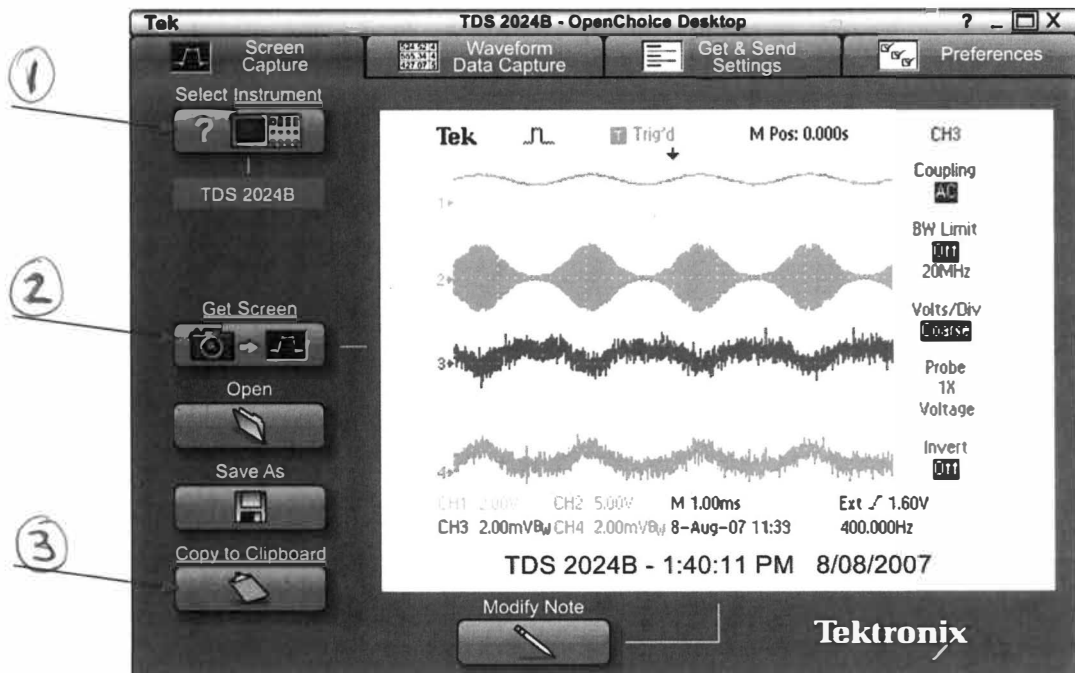
Acousto-Optics

- 1) Software and device operation manual** – Description.
- 2) Model AOD-70 acousto-optic light deflector (IntraAction Corp)** – Description and operation.
- 3) Model 1206C acousto-optic modulator (Isomet Corp)** – Specification and principles.
- 4) The acousto-optic effect** – extract from “Optoelectronics: an introduction”, J. Wilson and J.F.B. Hawkes, 2nd edition (1983).
- 5) Fundamentals of acousto-optics** – R.P. Main, Lasers and Applications, June 1984, pp 111-116.
- 6) Experiments in the interaction of light and sound for the advanced laboratory** – D.T. Pierce and R.L. Byer, Am. J. Phys 41 (1973) 314.

1) Software and device operation manual

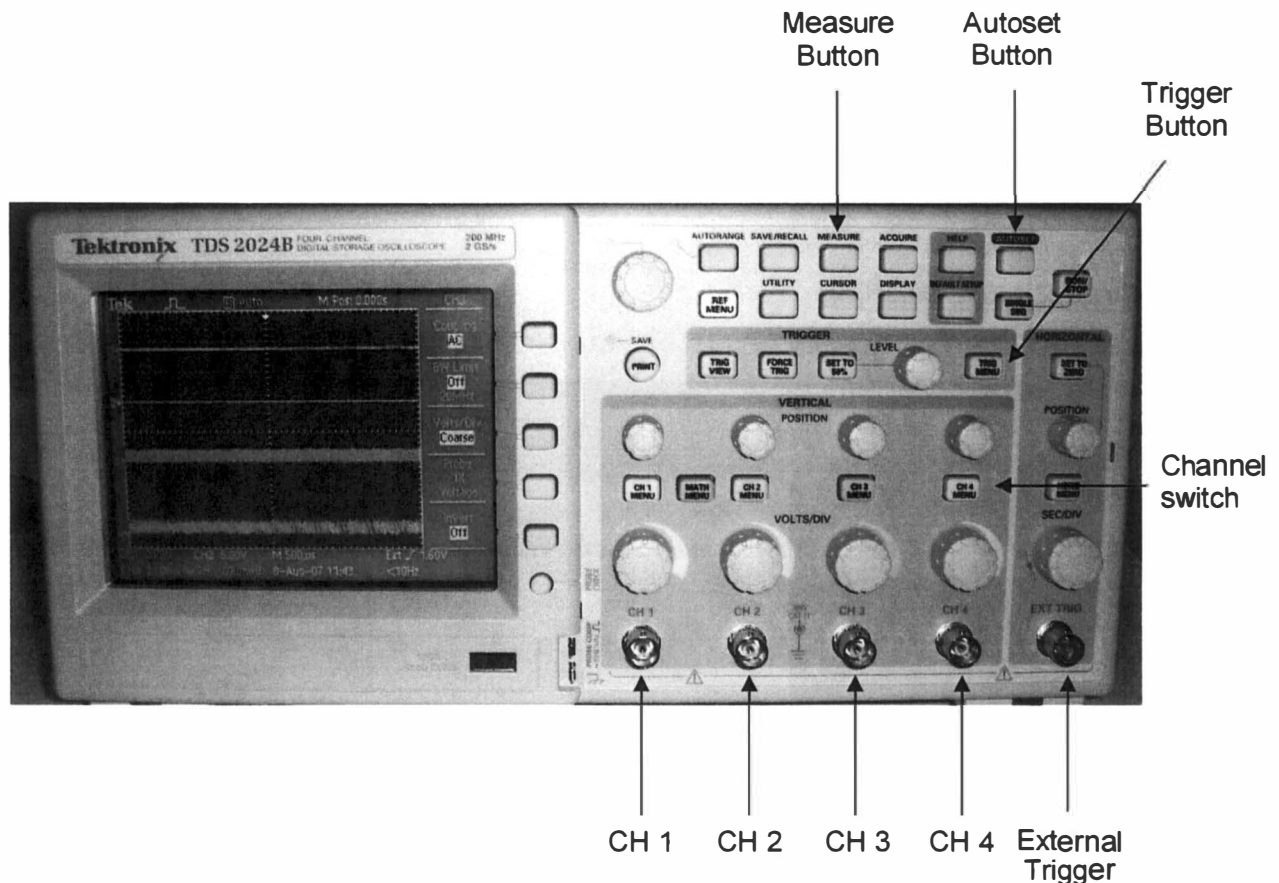
Software:	OpenChoice Desktop	p. 1
Devices:	Tektronix TDS 2024B (4-Channel Oscilloscope (DSO))	p. 2
	GW Function Generator Function Generator SFG-1003	p. 3
	GW GSG-120 (FM/AM Signal Generator)	p. 4
	Digitech QM-1462 (Multimeter)	p. 5

OpenChoice Desktop



1. Press the Icon 'Select Instrument' to connect to the DSO. Choose the device on the USB port and press 'OK'.
2. Use the 'Get Screen' button to get the current picture on the DSO.
3. Use 'Copy to Clipboard' and paste the picture into WORD.

Tektronix TDS 2024B 4-Channel Oscilloscope (DSO)



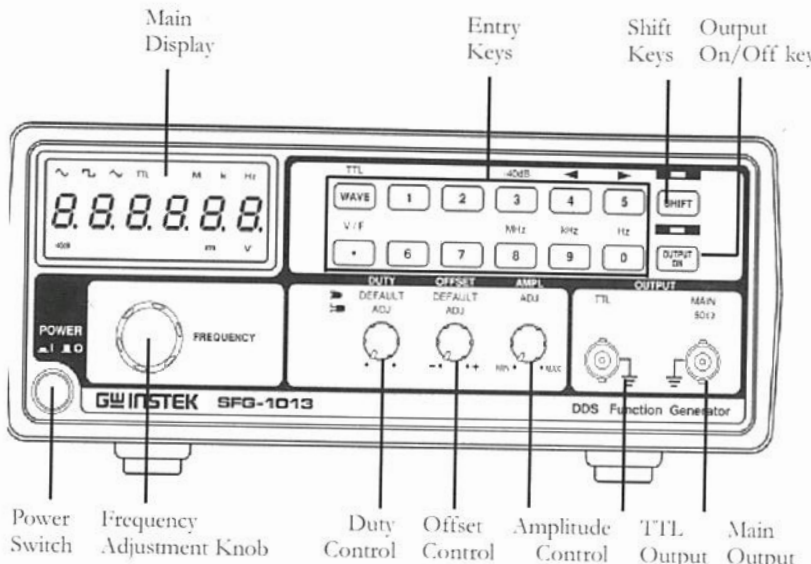
The easiest way to find the signals on the different Inputs (CH 1 – 4) is to use the AUTOSET button.

To switch on/off the channels you have to press the Channel switches you want.

To select a signal for triggering, the TRIG MENU button must be pressed. On the right side of the screen appears at the second button from the top a field which says 'Source'. By repeatedly pressing the button the source can be changed. There are two main variations of triggering. You can either use one of the channel signals or an external trigger signal.

The knobs over the BNC inputs of the channels can be used to change the voltage per division (vertical scale) of the associated signal. The knob over the BNC input of the external trigger signal changes the seconds per division (horizontal scale).

Front Panel



Main Display

7 segment LED



Shows frequency and voltage.

TTL indicator



Indicates that the TTL output is enabled. For details, see page25.

Waveform indicator



Indicates the waveform shape: Sine, Square, and Triangle.

Frequency indicator



Indicates the output frequency: MHz, kHz, or Hz.

Voltage indicator
SFG-1013 only)



Indicates Voltage unit: mV, or V. For voltage measurement detail, see page22.

-40dB indicator
SFG-1013 only)



Indicates -40dB attenuation is activated. For details, see page22.

Entry keys

Waveform key



Selects the waveform: sine, square, and triangle. For details, see page20.

TTL activation



Activates TTL output. For details, see page25.

Numerical keys

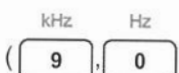


Specifies frequency.

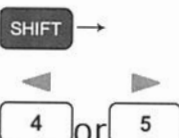
Frequency unit selection



Specifies the frequency unit: MHz, kHz, or Hz.



Cursor selection



Moves the cursor (frequency editing point) left or right. For details, see page21.

-40dB attenuation
(SFG-1013 only)



Attenuates amplitude by -40dB. For details, see page22. Key operation is for SFG-1013 only.

Frequency /
Voltage display
selection
(SFG-1013 only)



Switches the display between frequency and voltage. For details, see page22. For SFG-1013 only.

Shift key



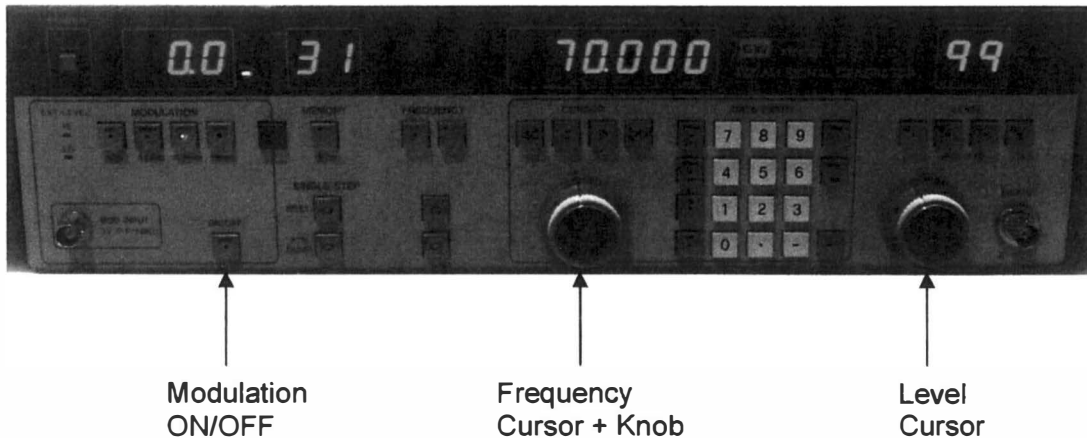
Selects the 2nd function associated to the entry keys. The LED lights when Shift is activated.

Output On/Off key



Turns the output On/Off. The LED lights when the output is On.

Good Well GSG-120 (FM/AM Signal Generator)



The *modulation* can be switched on or off. For this experiment it has to be OFF.

You can set the required **frequency** with the frequency knob and the arrow buttons. Don't use the keypad!

The *output level* should always be the maximum of 99 dB. To set this, you can either just use the knob and wind it up or if it is very low, press the level button D and wind it up to the maximum.

Digitech QM-1462 (Multimeter)

Button to
change
between
AC and
DC
mode



MODEL AOD-70

ACOUSTO-OPTIC LIGHT DEFLECTOR

Purpose of the Equipment

The Acousto-optic Light Deflector, Model AOD-70, is used to randomly position, or continuously scan a laser light beam at rates up to 20 KHz or greater. It has a capability of 400 spot resolution by the Rayleigh Criterion for a uniformly illuminated aperture. In addition to its function as a deflector, it may also be used for intensity modulation, strobing, doppler frequency shifting, and multiple beam generation. Two Deflectors can be cascaded with appropriate optics for two-dimension deflection.

Description

The AOD-70 is an all solid state acousto-optic light deflector manufactured from high quality flint glass as the interaction medium with Indium bonded Lithium Niobate piezoelectric transducers for generating the acoustic waves. The usable optical wavelength range is from 420 to 700 nm with 633 nm the design wavelength. A light beam entering the sound field at nearly normal incidence is deflected at an angle proportional to the acoustic frequency. A frequency deviation of 40 MHz centered at 70 MHz will deflect 633 nm light through an angle of 6.5 milliradians centered 11.4 milliradians from the undeflected beam. Since the Deflector utilizes a "phased array beam steering technique," the deflected light will have nearly constant intensity across the deflection angle.

Resolution depends on the time bandwidth product which is determined by the length of the optical aperture and bandwidth of the transducers. With a 39 mm aperture (10 μ sec) and a transducer bandwidth of 40 MHz, 400 spots of resolution are achieved. The maximum aperture of 39 mm represents a transit time of 10 μ sec. This is the time it takes to clear the sound from the optical aperture and is thus the switching time in a random access, 400 spot system. A trade off exists between resolution and access time - the smaller the beam width, the faster the access time, with correspondingly less resolution.

Signal Source (Driver)

The signal source required to drive the Deflector is a variable frequency generator with power output capability of 4 watts into a 50 ohm load with a minimum frequency capability of 50 to 90 MHz. The output power characteristic should have a positive 2 db slope from 50 to 90 MHz because of the frequency dependence of acoustic attenuation in the Deflector. The output impedance should be 50 ohms.

Interconnecting Cable

The coaxial cable which connects the Deflector to the driver should be selected to be a nominal one-quarter wavelength transmission line at the center frequency of 70 MHz. The cable should have a characteristic impedance of 50 ohms.

Modes of Operation. Deflection Mode

The angle between the deflected and undeflected beam is dependent upon the light wavelength and the acoustic frequency $\alpha = 0.26 \times \lambda \times f$. The total deflection angle of 6.5 milliradians is proportional to the total frequency deviation $\Delta f = 40$ MHz, the angle being limited by the piezoelectric transducers which act electrically as a bandpass filter. The intensity of the deflected light is proportional to acoustic power.

The Rayleigh limit resolution, N, is defined as the total deflection angle divided by the angular spot size. The relation simplifies to $N = \tau \times \Delta f$, where τ is the acoustic transit time across the optical aperture. Transit time $\tau = 2.56 D\mu\text{sec}$ (D the optical aperture in cm) is the time necessary to establish a new frequency in the optical beam. Therefore, in a random access application it is the minimum switching time, or in a scanning application it is the retrace time. The Deflector has a Rayleigh resolution capability of 400 spots based on a Δf of 40 MHz and a maximum τ of 10 μsec ($D = 3.9$ cm). However, to fill the full optical aperture of 3.9 cm anamorphic optics such as cylinder lenses or cylinder telescopes should be used.

Intensity Modulation Mode

When used as intensity modulator the RF input frequency to the Deflector is held constant while the signal amplitude is varied to produce intensity modulation of the laser beam. The relation between light intensity and applied voltage to the Deflector, as in any acousto-optic device, is not linear but is $I \propto \sin^2 kV$, where k is a constant and V is applied voltage. It is therefore necessary to incorporate a gamma correction circuit in the RF driver to linearize the input-output characteristics if desired.

Modulation bandwidth is inversely proportional to optical beam diameter. Depth of modulation as a function of frequency and beam diameter is given by $e^{-(f/f_e^2)}$, where $f_e = 3.45/D$ MHz (D expressed in mm) and f is modulation frequency in MHz. Thus a 0.65 mm beam will have a 50% depth of modulation at 4.5 MHz, increasing to 100% at dc. The light wavelength does not affect modulation frequency

response, although the acoustic power needed to diffract a given light percentage is proportional to the square of the light wavelength.

Diffraction efficiency - the percentage of incident light diffracted into the first main order - is also dependent upon beam diameter. Efficiency is 85% for a 633 nm, 1.4 mm diameter beam, and 80% for a 0.65 mm diameter beam.

Intensity modulation appears on both the diffracted and undiffracted light, one being the inverse of the other. A 100% depth of modulation cannot be obtained with the undiffracted beam, while a contrast ratio in excess of 1000:1 is possible with the diffracted beam.

Strobing Mode

Light chopping or strobing can be accomplished by the application of a pulsed RF signal. The general considerations for the pulse repetition rate in this mode of operation are as specified for Intensity Modulation. The rise time T_r (10% to 90% intensity) is given by $T_r = 0.65\tau$ where $\tau = D \times 0.26 \mu\text{sec}$ when D is the optical beam diameter at the $1/e^2$ intensity points and is given in mm.

Doppler Shift Modulation Mode

Acousto-optic devices have the property that the frequency of the diffracted light, is either up-shifted or down-shifted by the frequency of the acoustic wave. The undiffracted light is not shifted and can be used e.g. as the local oscillator for optical heterodyne detection. The Deflector is capable of changing the frequency of the diffracted light 50 to 90 MHz. When the optical beam enters the Deflector in a direction opposite to the direction of sound travel, the light is up-shifted. Light is down-shifted for the other case where the two directions coincide.

Multiple Light Beam Generation Mode

The high frequency sound waves generated in the Deflector produce a three dimensional diffraction grating with a spacing dependent on the frequency of the sound. The angle of the diffracted light is proportional to the optical wavelength and inversely proportional to the acoustic wavelength. If several frequencies are applied to the Deflector, several diffracted light beams will be created.

Inspection

Check the optical glass surface for the presence of dust, lint, or fingerprints. Dust and lint can be removed with a camel's hair brush, or by directing a stream of dry compressed gas across the surface. If fingerprints are observed clean the glass surfaces using standard approved solvents and methods for cleaning high quality optical

glass. Although the surfaces have a hard multilayer dielectric antireflection coating, care should be taken not to scratch the surfaces.

Mounting

The Deflector can be mounted in any orientation by four 4-40 machine screws placed 90° apart on the 1-1/4 inch bolt circle. Maximum screw depth is 0.200 inches. The center of the bolt circle is the center of rotation for the optical aperture. The scanning light beam can be either to the right or left or zeroth order depending on Deflector orientation. (See figure 1-2).

Alignment

Initially, the mounting system must provide adequate adjustment to facilitate locating the light beam in the center of the optical aperture. Alignment is accomplished by means of the test set up shown in figure 1-3. The Deflector should be connected to the Model DE-70 VCO Deflector Drive by the supplied coaxial cable. To reduce the possibility of misalignment due to acousto-optic saturation effects, the electrical drive power should be lower than that required for maximum light diffraction. The proper drive level will initially be set at the factory. While sweeping the Deflector in the range of approximately 50 to 90 MHz and observing the light output on the oscilloscope, an optimally flat light vs. frequency response can be obtained by rotating the Deflector to locate the most satisfactory Bragg angle. Optimum output intensity is obtained by aligning the optical beam parallel to the sound field and adjusting the vertical position to assure that the total optical beam is in the sound field. Maximally flat light response and bandwidth can then be obtained by increasing the drive power to the proper level. The response obtained at the factory is given by figure 1-4.

NOTE

TAKE CARE THAT THE LASER DOES NOT SATURATE
THE PHOTODETECTOR

ACOUSTO-OPTIC MODULATOR

May, 1981

SPECIFICATIONS

Spectral Range:	488-633nm*
Interaction Medium:	Lead Molybdate ($PbMoO_4$)
Acoustic Velocity:	3.63mm/ μ s
Active Aperture:	1mm
Center Frequency (CF):	110MHz
Input Impedance:	50Ω nominal
Input VSWR:	<1.5:1 @ 110MHz
Optical Power Density:	250W/mm ² focussed
DC Contrast Ratio:	>1000:1

PERFORMANCE VS. WAVELENGTH

Wavelength** (nm):	488	515	633
RF Drive Power (W):	<0.5	<0.5	<1.0
Bragg Angle (mr):	7.4	7.8	9.6
Beam Separation (mr):	14.8	15.6	19.2
Static Insertion Loss (%):	<5	<3	<3

PERFORMANCE VS. BEAM DIAMETER

Beam Diameter (mm):	1.0	0.34	0.2	0.084
Rise Time*** (ns):	180	60	35	15
Video Bandwidth (MHz):	2	6	10	25
Deflection Efficiency (%):	>85	>85	>80	>60

* On special order, the modulator may be supplied for use at 442nm. Static insertion loss: <10% at 442nm.

** Either Vertical or Horizontal polarization may be used.

*** Typical values with TEM_{00} Gaussian Beam Profile.

The typical MTF (depth of modulation) curve for the 1206C modulator, assuming a .084mm beam diameter, is shown at the left. For larger beam diameters the abscissa scales linearly. The curve is closely approximated by the function:

$$M \approx \exp - (f/f_o)^2$$

where

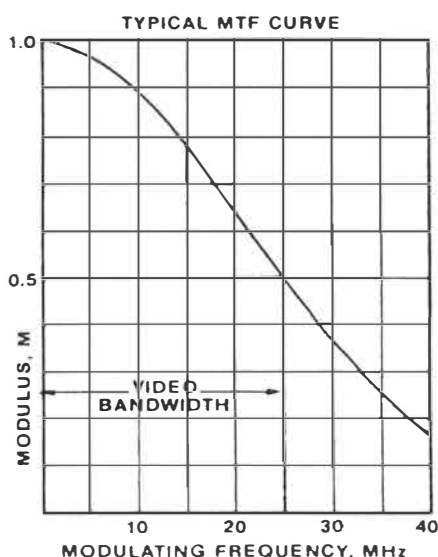
f = modulating frequency in MHz

f_o = parameter of modulator related to beam waist diameter = 30MHz (from experimental data)

The value of M from the curve may be used to determine the sine wave contrast ratio at a particular modulating frequency according to the relation:

$$CR = \frac{1 + M}{1 - M}$$

For digital, on-off modulation, the contrast ratio will be greater than the value calculated from the above equation.



3. PRINCIPLES OF ACOUSTO-OPTIC MODULATION

Figure 4 is a schematic representation of an acousto-optic modulator showing the input and output laser beams and the acoustic geometry. When an electrical voltage at the carrier frequency is applied across its top and bottom electrodes, the piezo-electric transducer generates an acoustic (ultrasonic) compression wave which travels down the interaction medium at a characteristic velocity, v . In lead molybdate $v = 3630 \text{ m/s}$.

When a laser beam is passed through the interaction medium more or less at right angles to the acoustic energy flow, the compression wave behaves like a diffraction grating. As in a diffraction grating, maximum light is diffracted into the first order beam (I_1), when the incoming beam enters the grating at a slight angle off normal, called the Bragg angle, where the Bragg angle is given by the equation:

$$\theta \approx \frac{\lambda f}{2v}$$

where

θ = Bragg angle

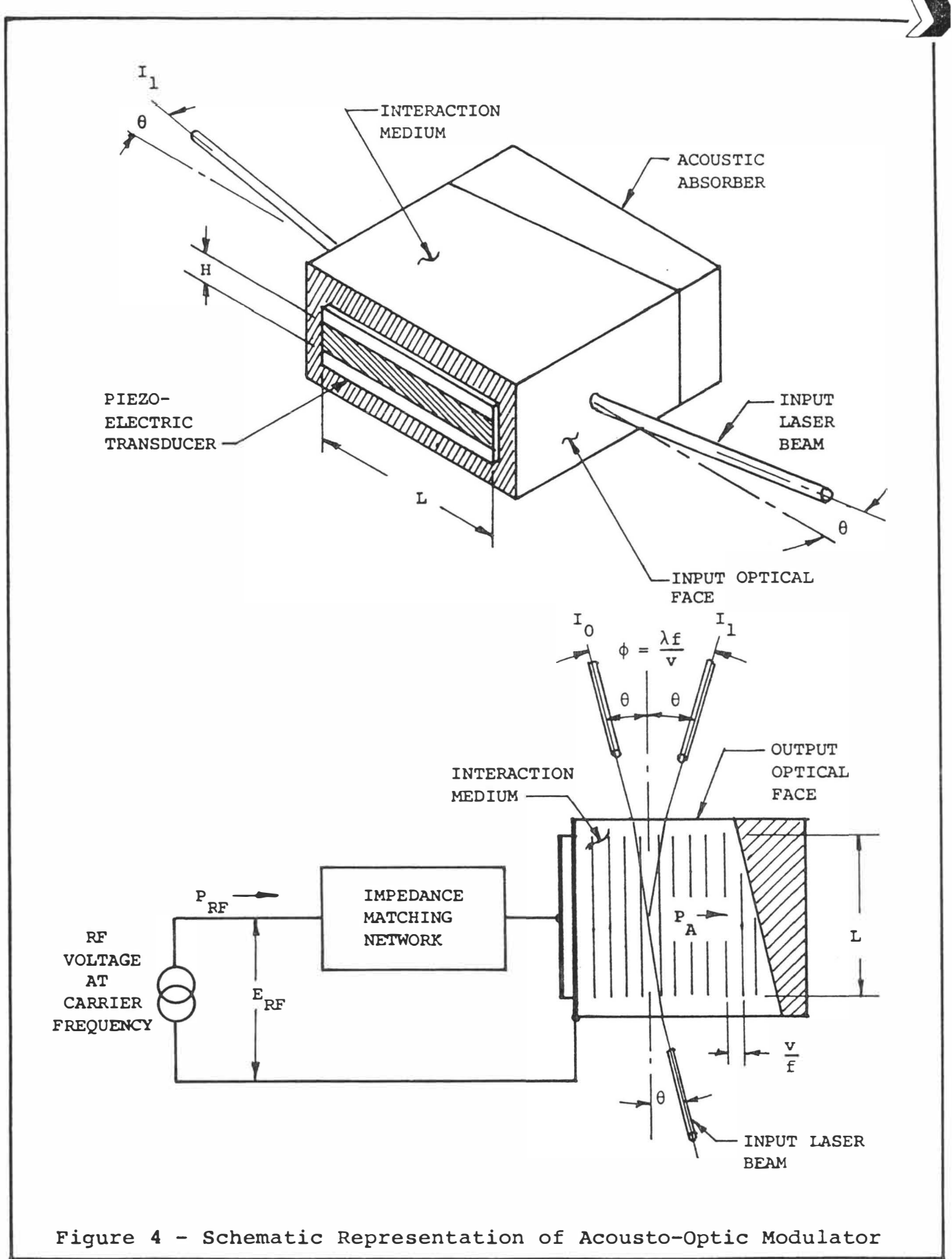
λ = laser wavelength

f = ultrasonic center frequency

v = acoustic velocity

In the usual arrangement, the input and output faces of the interaction medium are parallel. Therefore, when there is no acoustic energy in the medium, all of the laser light which enters the medium exits from the opposite face at the same Bragg angle. Inside the medium, of course, the angles are reduced by the index of refraction of the medium according to Snell's law. Nonetheless, the symmetry is maintained.

As the acoustic energy is increased from zero, some of the laser light is diffracted into the first order beam (I_1) direction and some remains in the zeroth order beam. The angle ϕ between the



first and zeroth order beam is twice the Bragg angle, and is

$$\phi = \frac{\lambda f}{v}$$

The amount of light which is diffracted into the first order beam is given by the equation:

$$\xi = \frac{I_1}{I_0} = \sin^2 \frac{\pi}{2} \sqrt{\frac{2M_2 L P_{ac}}{\lambda^2 H}}$$

where

ξ = diffraction efficiency

I_1 = light intensity in the first order beam

I_0 = light intensity in the zeroth order (straight-through) beam with no acoustic energy applied to the interaction medium

λ = laser wavelength

M_2 = photoelastic figure of merit of the medium
= $36 \times 10^{-15} m^2/\text{watt}$ for lead molybdate

L = length of the photoelastic interaction

H = width of the acoustic column (i.e., width of top electrode)

P_{ac} = acoustic power in the interaction medium

Since M_2 , L , and H are fixed parameters of the particular acousto-optic modulator design and since the acoustic power is equal to the RF input power (P_{RF}) times a proportionality constant, the preceding equation may be rewritten as:

$$\xi = \frac{I_1}{I_0} = \sin^2 \frac{k}{\lambda} \sqrt{P_{RF}}$$

Further, since $P_{RF} = E_{RF}^2 / R$ for an impedance-matched transducer, the above equation may be simplified to:

$$\xi = \frac{I_1}{I_0} = \sin^2 \frac{k E_{RF}}{\lambda}$$

Owing to the \sin^2 relationship, efficiency reaches a peak value, called saturation, for a particular acoustic power level $P_{SAT} = \lambda^2 H / 2M_2 L$. When the acoustic power is increased beyond saturation, the efficiency diminishes. Note that P_{SAT} is wavelength dependent. In a given modulator the shorter the wavelength, the lower the saturation power.

Figure 5 is a family of efficiency vs. voltage curves for the Models 1205-1-1, 1206-1 and 1209 acousto-optic modulators. In these devices the conversion factor between electrical input power to acoustic power is approximately 0.5 and the input impedance is very nearly resistive at 50Ω . The corresponding values of saturated RF input power and RF input voltage for these devices at various wavelengths are shown in the table below:

<u>Model</u>	<u>Wavelength</u>	<u>Saturated RF Power (watts)</u>	<u>Saturated RF Voltage (RMS)</u>
1205-1-1	442	0.5	5.0
	488	0.58	5.4
	515	0.65	5.7
	633	1.0	7.1
1206-1	442	0.8	6.3
	488	0.95	6.9
	515	1.0	7.1
	633	1.6	8.9
1209	633	1.0	7.1

To intensity modulate a laser beam digitally in an acousto-optic modulator requires that the RF carrier voltage (power) be varied between two states--zero and saturation. When the RF power applied to the modulator is zero, the light diffracted into the first order beam is zero. When the RF power applied to the modulator is at saturation, nearly all of the light is diffracted into the first order beam.

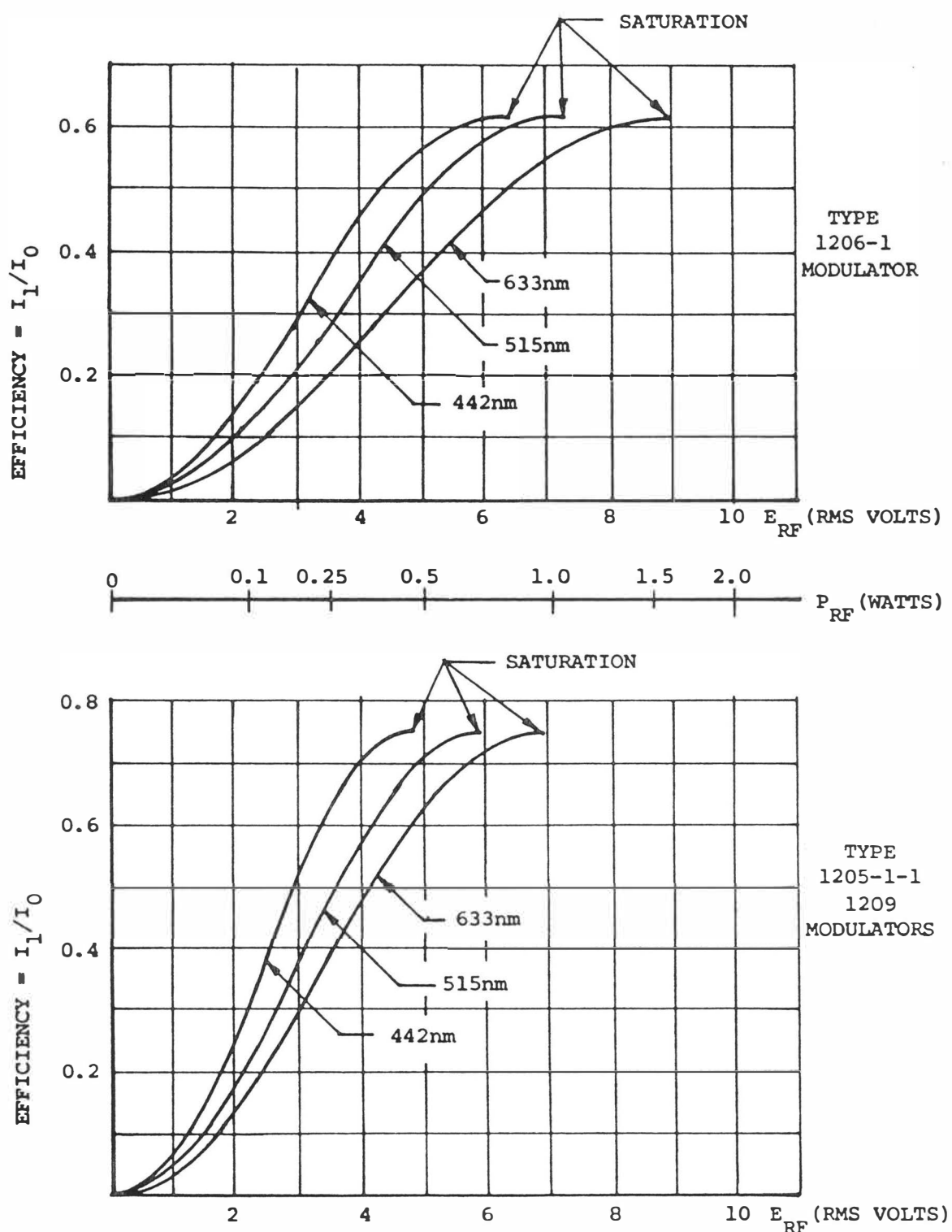


Figure 5 - Efficiency vs. Drive Voltage Curves (Typical)

Figure 6 shows the intensity vs. RF envelope voltage transfer function of the acousto-optic modulator in normalized units with the typical waveforms superimposed. It will be noted that the driving RF waveform is an on-off gated carrier. In effect, the acousto-optic interaction demodulates the RF carrier, transforming the modulation envelope (digital data stream) into intensity variation of the first order diffracted laser beam.

Digital rise time of an acousto-optic modulator is mainly determined by the parameters of the modulator itself. With no RF power applied, all light rests in the zeroth order beam. A short time after RF power is applied to the modulator, the leading edge of the acoustic pulse reaches the laser beam position and begins to switch light from the zeroth order to the first order beams. For an input laser beam of circular cross section and Gaussian profile, the 10% to 90% switching time (rise time) is $0.65 \times$ time required for the acoustic beam to traverse the laser beam, to a first approximation. That is $t_r \approx 0.65\tau = 0.65(d/v)$ where d is the laser beam diameter in the modulator and v is the acoustic velocity.

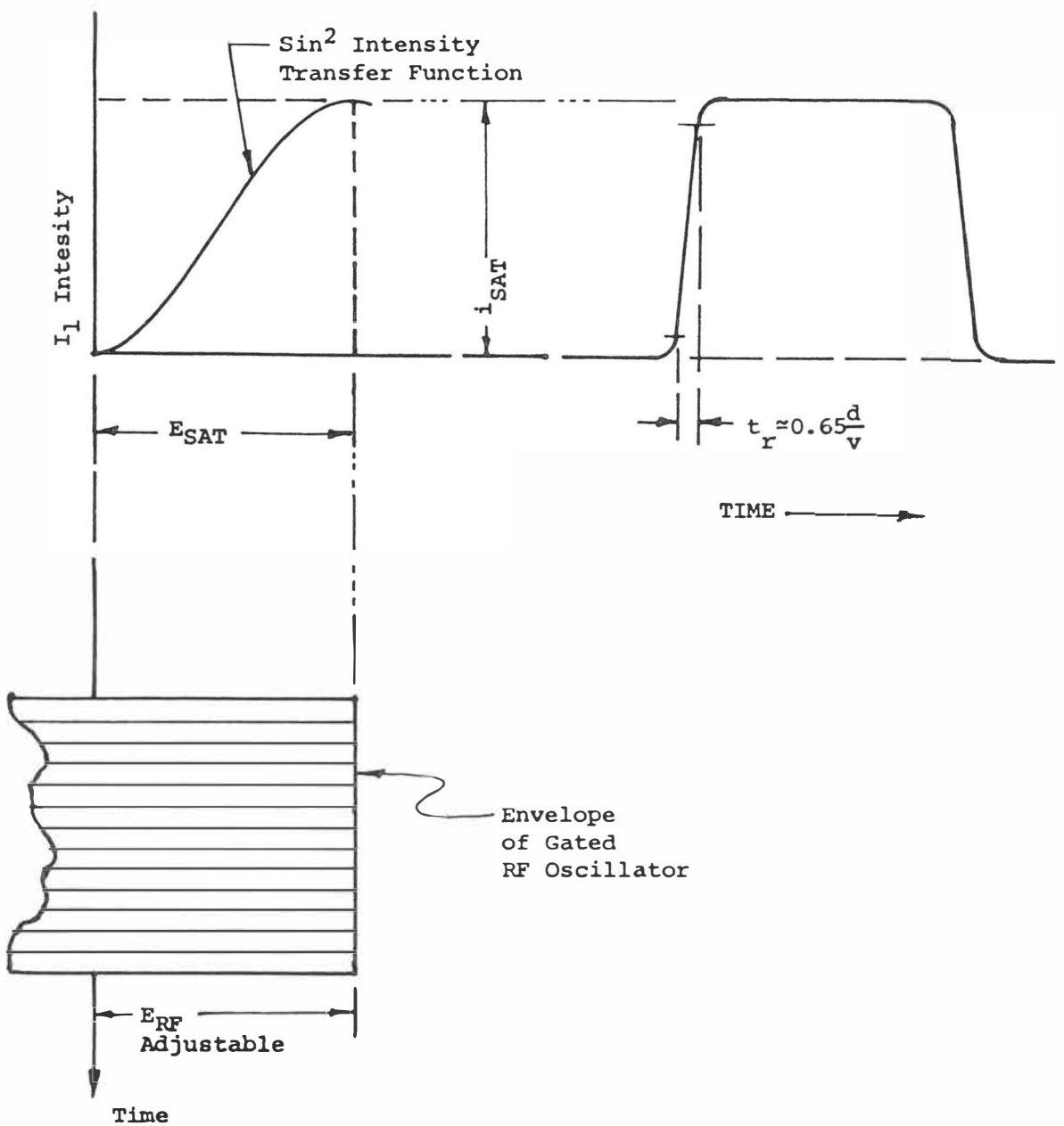


Figure 6, Intensity vs. RF Envelope Voltage Transfer Function

Table 3.3 Typical values of the Verdet constant V for $\lambda = 589.3 \text{ nm}$

Material	$V (\text{rd m}^{-1} \text{T}^{-1})$
Quartz (SiO_2)	4.0
Zinc sulfide (ZnS)	82
Crown glass	6.4
Flint glass	23
Sodium chloride (NaCl)	9.6

magnetic field. Faraday found (1845) that when a beam of plane polarized light passes through a substance subjected to a magnetic field, its plane of polarization is observed to rotate by an amount proportional to the magnetic field component parallel to the direction of propagation. This is very similar to optical activity which, as we saw in section 3.3, results from certain materials having different refractive indices n_r and n_l for right and left circularly polarized light. There is one important difference in the two effects. In the Faraday effect the sense of rotation of the plane of polarization is independent of the direction of propagation. This is in contrast to optical activity where the sense of rotation is related to the direction of propagation. Thus in the case under discussion the rotation can be doubled by reflecting the light back through the Faraday effect device.

The rotation of the plane of polarization is given by

$$\theta = VBL \quad (3.18)$$

where V is the Verdet constant (see Table 3.3 for some representative values), B is the magnetic flux parallel to the direction of propagation and L is the path length in the material. The Faraday effect is small and wavelength dependent; the rotation for dense flint glass is $\theta \approx 1.6^\circ \text{ mm}^{-1} \text{ T}^{-1}$ at $\lambda = 589.3 \text{ nm}$.

We can also express θ in terms of the refractive indices n_r and n_l , i.e.

$$\theta = \frac{2\pi}{\lambda} (n_r - n_l)L$$

A Faraday rotator used in conjunction with a pair of polarizers acts as an optical isolator which allows a light beam to travel through it in one direction but not in the opposite one. It may therefore be used in laser amplifying chains to eliminate reflected, backward traveling waves, which are potentially damaging. The construction of a typical isolator is shown in Fig. 3.18.

Light passing from left to right is polarized in the vertical plane by polarizer P_1 . The Faraday rotator is adjusted to produce a rotation of 45° in the clockwise sense. The second polarizer P_2 is set at 45° to P_1 so that it will transmit light emerging from the rotator. However, a beam entering from the right will be plane polarized at 45° to the vertical by P_2 and then have its plane rotated by 45° in the clockwise sense by the rotator. It will therefore be incident on P_1 with its plane of polarization at right angles to the plane of transmission and be eliminated. The device thus isolates the components on its left from light incident from the right.

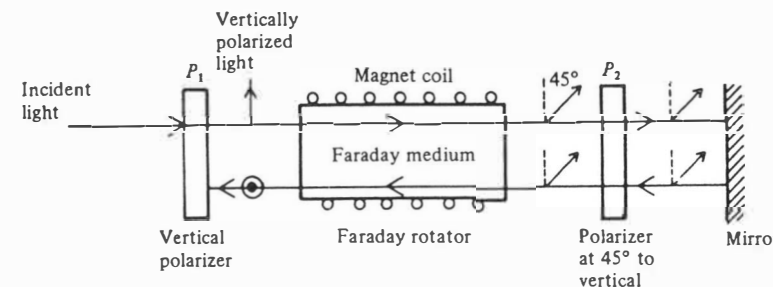


Fig. 3.18 Optical isolator based on the Faraday effect. The reflected ray is shown displaced for clarity.

One potential application of magneto-optics currently receiving attention is large capacity computer memories. Such memories must be capable of storing very large amounts of information in a relatively small area and permit very rapid readout and, preferably, random access. The usual magnetic memories have a number of limitations of size and reading speed. Optical techniques can overcome both these constraints (refs. 3.4).

The magneto-optic memories developed so far are read via the Faraday effect or the magnetic Kerr effect, which relates to the rotation of a beam of plane polarized light reflected from the surface of a material subjected to a magnetic field. In either case a magnetized ferro- or ferrimagnetic material rotates the plane of polarization of laser light incident on it.

Writing may be achieved by heating the memory elements on the storage medium to a temperature above the Curie point using a laser beam. The element is then allowed to cool down in the presence of an external magnetic field thereby acquiring a magnetization in a given direction. Magnetizations of the elements in one direction may represent 'ones', in the opposite direction 'zeros'. To read the information the irradiance of the laser beam is reduced and then directed to the memory elements. The direction of the change in the polarization of the laser beam on passing through or being reflected from the memory elements depends on the directions of magnetization; therefore we can decide if a given element is storing a 'one' or 'zero'.

Prototype systems, incorporating, for example, a 50 mW He-Ne laser with a Pockels modulator and manganese bismuth (MnBi) thin film storage elements, have enabled information to be stored, read and erased at rates in excess of 1 Mb s^{-1} .

3.8 Acousto-optic effect

The acousto-optic effect is the change in the refractive index of a medium caused by the mechanical strains accompanying the passage of an acoustic (strain) wave through the medium. The strain and hence the refractive index varies periodically with a wavelength Λ equal to that of the acoustic wave. The refractive index changes are caused by

the photoelastic effect which occurs in all materials on the application of a mechanical stress. It can be shown that the change in refractive index is proportional to the square root of the total acoustic power (ref. 3.5).

In general, the relationships between changes of refractive index and mechanical strain, and between the strain and stress are rather complicated (ref. 3.6). However, for simplicity we can consider the case of a monochromatic light wave, wavelength λ , incident upon a medium in which an acoustic wave has produced sinusoidal variations of wavelength Λ in the refractive index. The situation is shown in Fig. 3.19, where the solid horizontal lines represent acoustic wave peaks (pressure maxima) and the dashed horizontal lines represent acoustic wave troughs (pressure minima). As the light enters the medium, the portions of the wavefront near to a pressure peak will encounter a higher refractive index and therefore advance with a lower velocity than those portions of the wavefront which encounter pressure minima. The wavefront in the medium therefore soon acquires the wavy appearance shown by the dashed curve in Fig. 3.19. The acoustic wave velocity is very much less than the light wave velocity, so we may ignore it and consider the variation in refractive index to be stationary in the medium.

As elements of the light wave propagate in a direction normal to the local wavefront, almost all the wave elements will suffer a change in direction leading to a re-distribution of the light flux, which tends to concentrate near regions of compression. In effect, the

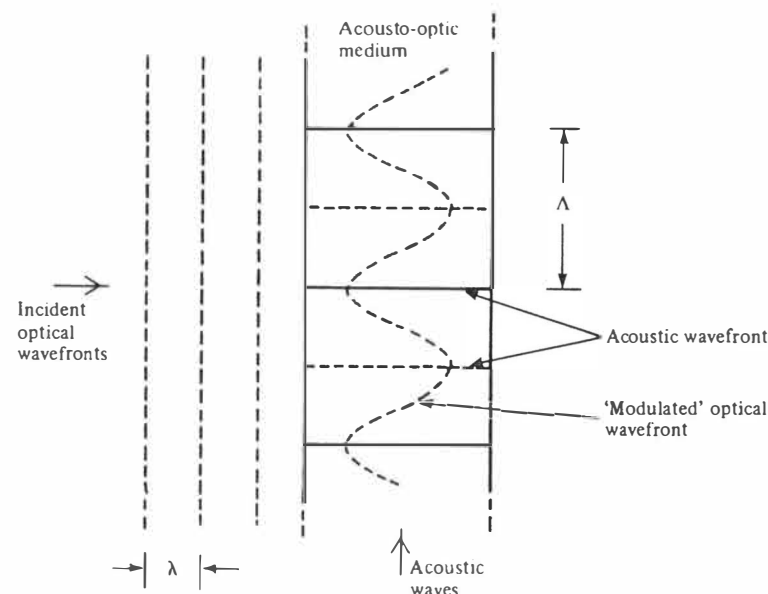


Fig. 3.19 Schematic illustration of acousto-optic modulation. The acoustic waves change the refractive index of the medium in a periodic way so that the plane optical wavefronts take on the 'wavy' appearance shown (very much exaggerated) as they propagate through the medium.

acoustic wave sets up a diffraction grating within the medium so that optical energy is diffracted out of the incident beam into the various orders. There are two main cases of interest, namely (a) the *Raman–Nath regime* and (b) the *Bragg regime*.

In the Raman–Nath regime, the acoustic diffraction grating is so 'thin' that the diffracted light suffers no further redistribution before leaving the modulator. The light is diffracted as from a simple plane grating such that

$$m\lambda_0 = \Lambda \sin \theta_m \quad (3.19)$$

where $m = 0, \pm 1, \pm 2, \dots$, is the order and θ_m is the corresponding angle of diffraction, as illustrated in Fig. 3.20.

The irradiance I of the light in these orders depends on the 'ruling depth' of the acoustic grating, which is related to the amplitude of the acoustic grating. This, in turn, is related to the amplitude of the acoustic modulating wave (that is, the stress produced). The fraction of light removed from the zero order beam is $\eta = (I_0 - I)/I_0$, where I_0 is the transmitted irradiance in the absence of the acoustic wave. Thus amplitude variations of the acoustic wave are transformed into irradiance variations of the optical beam.

The physical basis of the Bragg regime is that light diffracted from the incident beam is extensively re-diffracted before leaving the acoustic field. Under these conditions, the acoustic field acts very much like a 'thick' diffraction grating, that is, a grating made up of planes rather than lines. The situation is then very similar to that of Bragg diffraction (or 'reflection') of X rays from planes of atoms in a crystal. Consider a plane wavefront incident on the grating planes at an angle of incidence θ , as shown in Fig. 3.21(a); significant amounts of light will emerge only in those directions in which constructive

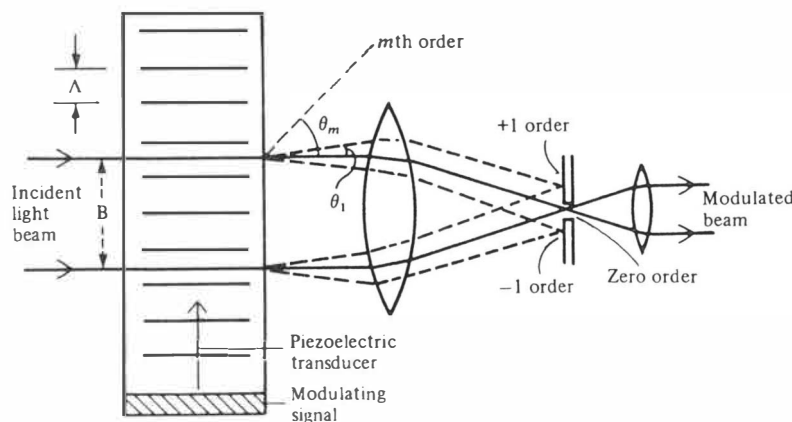


Fig. 3.20 Geometry for Raman–Nath (or transmission-type) acousto-optic diffraction grating modulation. The amount of light diffracted into the orders $m \geq 1$ from the incident beam, and hence the modulation of the transmitted beam, depends on the amplitude of the modulating signal.

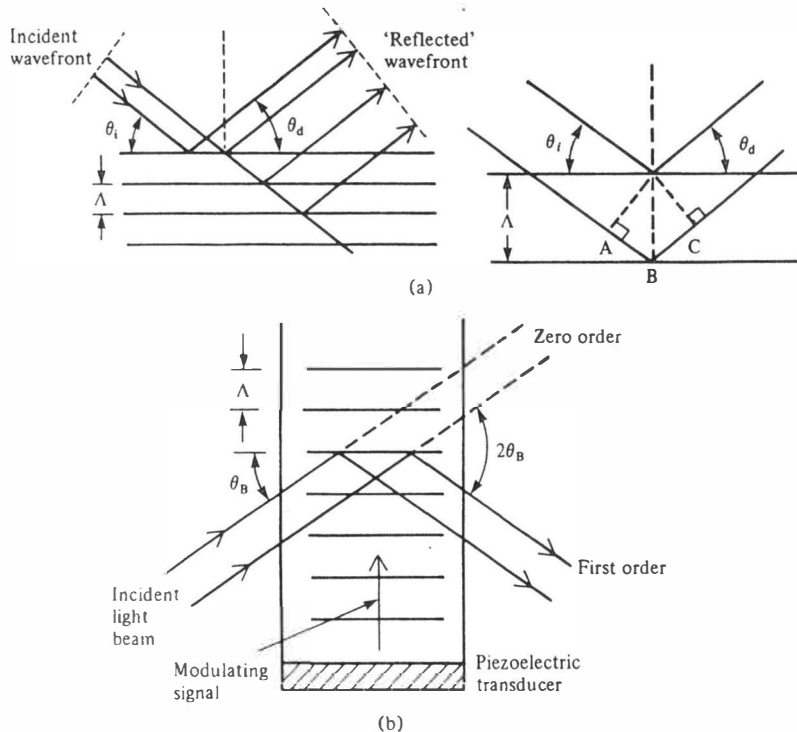


Fig. 3.21 Geometry for Bragg (or reflection-type) acousto-optic diffraction grating modulation: (a) incident rays being scattered from successive layers – for constructive interference the path difference $AB + BC$ must equal an integral number of wavelengths $m\lambda$ and (b) the amount of light 'reflected' into the first order depends on the amplitude of the modulating signal.

interference occurs. The conditions to be satisfied are: (a) light scattered from a given grating plane must arrive in phase at the new wavefront and (b) light scattered from successive grating planes must also arrive in phase at the new wavefront, implying that the path difference must be an integral number of wavelengths. The first of these conditions is satisfied when $\theta_d = \theta_i$, where θ_d is the angle of diffraction. The second condition requires that

$$\sin \theta_i + \sin \theta_d = \frac{m\lambda}{\Lambda}$$

with $m = 0, 1, 2, \dots$. The two conditions are simultaneously fulfilled when

$$\sin \theta_i = \sin \theta_d = \frac{m\lambda}{2\Delta} \quad (3.20)$$

The diffraction is similar to that obtained with a plane grating, but only for special angles of incidence; the angle of incidence must equal the angle of diffraction.

Although in the simplified theory given above strong scattering can take place when m is equal to any positive integer, a more rigorous treatment, taking into account the fact that scattering is not from discrete planes but from a continuous medium, shows that scattering only takes place when $m = 1$. This is shown in Fig. 3.21(b), the equation for the so-called Bragg angle θ_B then becomes $\sin \theta_B = \lambda/2\Delta$. The modulation depth $(I_0 - I)/I_0$ (or diffraction efficiency, η) in this case can theoretically equal 100% in contrast to about 34% for the Raman–Nath case. At the Bragg angle it is given by $\eta = \sin^2 \phi/2$, where $\phi = (2\pi/\lambda) (\Delta n L/\cos \theta_B)$, Δn being the amplitude of the refractive index fluctuation and L the length of the modulator (ref. 3.7).

The acoustic waves, which create the diffraction grating, are of course moving through the medium and, as a consequence, the diffracted wave behaves as if it had been reflected from a 'mirror' moving with the same velocity as the grating, and therefore appears to originate from a source moving at *twice* the mirror (or grating) velocity. Thus the frequency of the reflected beam is changed by the Doppler effect (see Section 5.7) and is given by

$$v' = v_0 (1 \pm 2v_a (c/n))$$

where $\pm v_a$ is the component of the velocity of the acoustic wave along (or away from) the original beam direction and n is the medium refractive index. The frequency shift is thus:

$$\Delta v = v' - v_0 = \frac{\pm 2v_0 v_a n}{c}$$

If the light is incident at an angle $\theta_i = \theta_d$ to the acoustic wave as shown in Fig. 3.21a, then $v_x = v_a \sin \theta_d$ where v_a is the acoustic wave velocity. The frequency shift is then:

$$\Delta v = \frac{\pm 2v_0 v_a \sin \theta_d n}{c} \quad (3.21)$$

Combining eqs. (3.21) and (3.20) and taking $m = 1$ gives a frequency shift of $\pm v_a/\Lambda$ or $\pm f_0$, where f_0 is the acoustic wave frequency. This change in frequency can be used as the basis of a frequency modulator.

The minimum time required to move from a condition where the acoustic wave interacts with the light beam and 'turns off' the undiffracted light to a condition where there is no diffraction is the transit time of the acoustic wave across the optical beam. This is simply, from Fig. 3.20, $t_{\min} = B/v_a$, where B is the optical beam width. Hence the bandwidth of the modulator is limited to about v_a/B . Commercial modulators have bandwidths of up to 50 MHz. This limitation is partly due to the frequency dependence of the acoustic losses of available acousto-optic materials. At the present time only LiNbO_3 and PbMoO_4 appear to have sufficiently low loss to have a reasonable prospect of being operated at appreciably higher frequencies.

Acousto-optic modulators can in general be used for similar applications to electro-optic modulators, though they are not so fast. On the other hand, because the electro-optic effect usually requires voltages in the kilovolt range, the drive circuitry for modulators based on this effect is much more expensive than for acousto-optic modulators, which operate with a few volts.

Example 3.4 Acousto-optic modulator

Given the following data for a PbMO_4 acousto-optic modulator, we may calculate the Bragg angle; the maximum change in refractive index of the material and the maximum width of the optical beam of wavelength 633 nm that may be modulated with a bandwidth of 5 MHz.

The modulator length is 50 mm, diffraction efficiency 70%, while the acoustic wavelength is 4.3×10^{-5} m and the acoustic velocity is 3500 m s⁻¹.

The angle of diffraction (from eq. 3.20) is

$$\theta_B = \sin^{-1} \left(\frac{633 \times 10^{-9}}{2 \times 4.3 \times 10^{-5}} \right) = 7.4 \text{ m rad (or } 0.42^\circ)$$

The value of ϕ is given by

$$\phi = 2 \sin^{-1} \sqrt{\eta} = 2 \sin^{-1} \sqrt{0.7}$$

$$\phi = 113.6^\circ$$

$$\therefore \Delta n = \frac{\phi \lambda \cos \theta_B}{2\pi L} = 1.27 \times 10^{-5}$$

The bandwidth is v_a/B and hence the maximum optical beamwidth B is

$$\frac{3500}{5 \times 10^6} = 0.7 \text{ mm}$$

3.9 Nonlinear optics

Practical applications of nonlinear optical effects have arisen as a direct consequence of the invention of the laser. The very high power densities made available by lasers have enabled several phenomena, which were previously regarded as theoretical curiosities, to be observed and exploited.

The explanation of nonlinear effects lies in the way in which a beam of light propagates through a solid. The nuclei and associated electrons of the atoms in the solid form electric dipoles. The electromagnetic radiation interacts with these dipoles causing them to oscillate which, by the classical laws of electromagnetism, results in the dipoles themselves acting as sources of electromagnetic radiation. If the amplitude of vibration is small, the dipoles emit radiation of the same frequency as the incident radiation. As the irradiance of the radiation increases, however, the relationship between irradiance and amplitude of vibration becomes nonlinear resulting in the generation of harmonics of the frequency of the radiation emitted by the oscillating dipoles. Thus frequency doubling or second harmonic generation and indeed higher order frequency effects occur as the incident irradiance is increased. The electric polarization (or dipole moment per unit volume) P can be expressed as a power series expansion in the applied electric field \mathcal{E} by

Optoelectronics

An introduction

Second edition

J. WILSON

J. F. B. HAWKES

*Department of Physics,
Newcastle upon Tyne Polytechnic*



PRENTICE HALL

New York London Toronto Sydney Tokyo Singapore

Fundamentals of Acousto-Optics

Interactions of Light and Sound Form the Basis for a Family of Laser Accessories

by Roger P. Main, European Correspondent

Many laser accessories are based on the interactions of light and sound — the essence of acousto-optics. Newcomers to the laser world sometimes are confused by the various devices and their similarities and differences. In this article, we'll review the physics of wave motion in various media, and then discuss some examples taken from everyday practice.

Light Waves

Light waves are transverse waves — the amplitudes of oscillation of the electric and magnetic field vectors are orthogonal to the direction of propagation of the waves, and to one another (Figure 1). The electric

field vector interacts with matter strongly; the magnetic vector normally interacts with matter very weakly.

Light waves can propagate in a perfect vacuum; they do not require matter to support the oscillations. The speed of light waves propagating in matter is

$$c = c_0/n \quad (1)$$

where c_0 is the speed of light in vacuum (roughly 3×10^8 m/s) and n is the refractive index of the material. For nearly all materials, n is a real number and has a value ranging from 1 to 6. The value often depends upon the wavelength of the light. For metals and lossy dielectrics, n is a complex number.

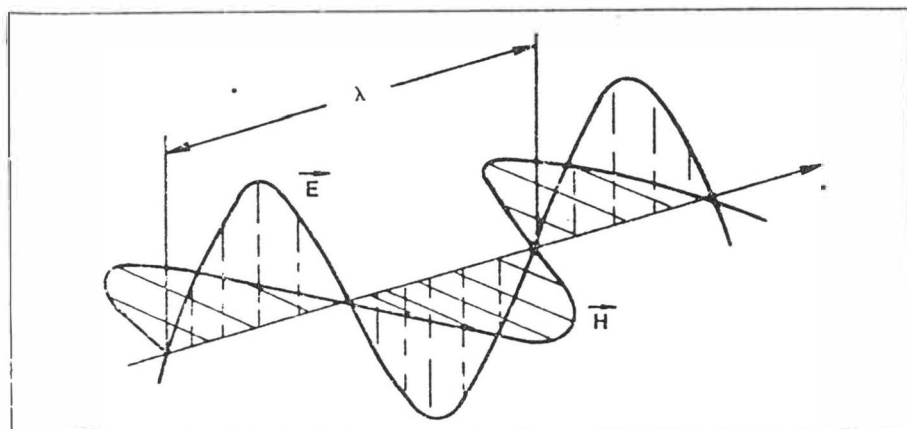


Figure 1. A light wave traversing free space.

Lasers & Applications June 1984

Sound Waves

In contrast with light waves, sound waves are longitudinal waves in matter — the directions of propagation and oscillation are the same. Matter (whether solid, liquid, gas, or plasma) must be present for sound waves to propagate. The amplitude of the waves is expressed in terms of the periodic compressions/rarefactions or strains/relaxations in the material. These take place in the direction of propagation (Figure 2). The distance between successive wavefronts is the wavelength of the sound wave. The speed of the sound waves is a complicated function of the properties (e.g., specific heat, mass density, strain modulus, etc.) of the material. Some representative values are given in Table 1.

The same relationships between wavelength (λ), frequency (ν), and speed (c) hold true for light and sound waves:

$$\begin{aligned} c &= \nu \lambda \\ c_s &= \nu_s \lambda_s \end{aligned} \quad (2)$$

Polarization

Light waves are transverse and may have polarization characteristics. These are specified in terms of the orientation of the electric and magnetic field vectors with respect

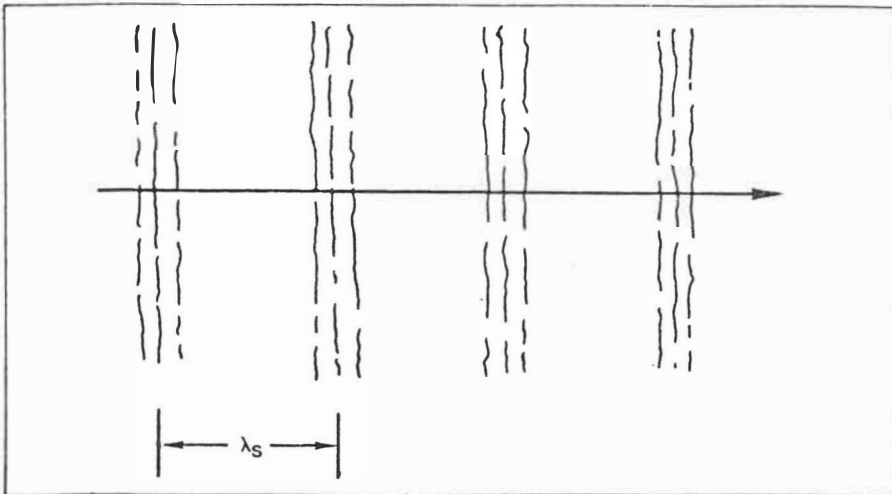


Figure 2. A sound wave traveling longitudinally through matter.

to an external reference frame, while remaining orthogonal to each other. As the wave propagates, these orientations may be fixed or variant.

Sound waves are longitudinal waves and, therefore, cannot have polarization characteristics. However, the interaction between light and sound waves will depend upon the polarization characteristics of the light wave and the orientation of its field vectors with respect to the direction of propagation of the sound wave, which may be changing in time. Why? The interaction occurs between the light wave (that is, the electric and magnetic field vectors which form it) and the structural lattice of the material itself, as influenced by the acoustic waves. These interactions are, in general, polarization-dependent.

The Mathematics of Acoustic Waves

An acoustic wave is a standing or traveling density modulation in a material. We may express this as a standing or traveling periodic variation in the quiescent state density, ρ_0 , of the material. Equation 3, below, shows the case of the traveling wave, which reduces to the standing-wave case by setting t equal to zero.

$$\rho - \rho_0 = \Delta \rho (x_1 t) \\ = \Delta \rho \sin (\omega_s t + k_s x) \quad (3)$$

where

$$\omega_s = 2 \pi \nu_s; k_s = 2 \pi / \lambda_s \quad (4)$$

These density modulations produce corresponding modulations in the refractive index of the material. In effect, Equation 3 can be restated as a change in the quiescent state refractive index of the material, n_0 , as

$$n - n_0 = \Delta n (x_1 t) \\ = \Delta n \sin (\omega_s t + k_s x) \quad (5)$$

In typical cases, $\Delta n/n_0$ is about 10^{-4} .

Table 1 — Approximate Values of the Speed of Sound in Various Materials

Material	Velocity (m/s)
Room Air	350
Water	1,500
Glass	3,100
Steel	4,800
Fused Silica (SiO_2)	6,000
Sapphire (Al_2O_3)	11,000

The interaction of light and sound was predicted theoretically by Brillouin in 1921 and demonstrated experimentally by Debye and Sears in 1932. The interaction produces a "scattering" of light waves from the sound waves. This scattering, the Debye-Sears effect, can be used to control or modulate the frequency, phase, amplitude (intensity equals the square of the amplitude), direction of travel, or angle of divergence (focus/defocus) of the light waves.

The scattering of light is produced by a modulation of the index of refraction of the material, caused by the disturbances of the sound waves (Figure 3). The transducer is a piezoelectric material (e.g., ZnO , LiNbO_3 , or BaTiO_3), which converts an input electrical signal into a mechanical displacement. If the electrical signal varies with time, so will the displacement.

A time-varying displacement in the transducer is coupled into the transparent material, producing periodic strains/compressions. These strains alter the density of the material in rhythm with the displacements of the transducer and

therefore with the electrical signal input to the transducer.

The modulations of the refractive index in the transparent material produce what can be compared to a "stack of glass plates," where the glass plates correspond to the acoustic wavefronts (Figure 4). Remember that

$$\lambda_s = C_s / \nu_s \quad (6)$$

For fused silica, $C_s = 6 \times 10^3 \text{ m/s}$. Let's assume $\nu_s = 1 \text{ MHz}$. Then λ_s will be 6 mm. If λ is 600 nm, then the ratio of λ_s to λ will be 10^4 .

Note that the glass plates may be either stationary (as would be the case for a standing sound wave) or moving (as would be the case for a traveling sound wave).

The Standing-Wave Case

Consider first the case of standing sound waves. For scattering (reflection) in a given direction to occur from a single plate, all parts of this plate must contribute in phase to the diffracted (reflected) energy in that direction (Figure 5). This means that the path difference

$$AE - BD = m\lambda \quad (7)$$

where m is any integer, positive, negative, or zero. By a simple application of geometry

$$x(\cos \Theta_i - \cos \Theta_R) = m\lambda \quad (8)$$

This can be satisfied for all points of the plate only if $m = 0$. Then

$$\Theta_i = \Theta_R \text{ (since } \Theta_i, \Theta_R \leq 90^\circ) \quad (9)$$

This is the well-known law of reflection, applied to standing acoustic waves.

For scattering in a given direction to occur simultaneously from all plates, the diffracted light from any two plates (acoustic wavefronts, to re-introduce the analogy) must interfere constructively along the direction of the diffracted beam (Figure 6). For constructive interference:

$$AO + OB = j\lambda \quad (10)$$

$$\lambda_s \sin \theta + \lambda_s \sin \Theta = 2\lambda_s \sin \theta = j\lambda$$

Here, j is either zero or a positive integer.

However, for maximum diffraction to occur, we must have $j = 1$ only. Remember, the refractive index modulation produced is slowly and continuously varying; it is not sharp

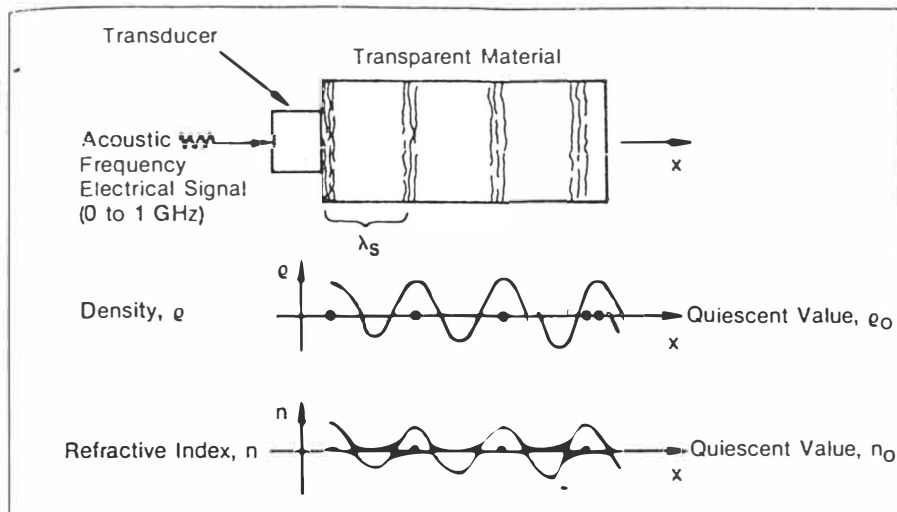


Figure 3. Periodic compressions/rarefactions in matter produced by an acoustic transducer generate periodic variations in the material's density and refractive index.

as we have idealized it. Values of j greater than 1 correspond to large angles, θ , for which the diffraction effect is weak, at best, in real cases. The value $j = 0$ corresponds to the case $\lambda_s = 0$, which is not of interest.

A quick sample calculation will yield interesting results. Let's assume a light wavelength of 500 nm, an acoustic frequency of 500 MHz, and sound speed of 6×10^3 m/s. Then

$$\begin{aligned}\lambda_s &= C_s / \nu_s = 1.2 \times 10^{-5} \text{ m} = 24 \lambda \\ \Theta &= \sin^{-1} \left[\frac{\lambda}{2\lambda_s} \right] = \sin^{-1} \left[\frac{1}{48} \right] \\ \Theta &\approx 1.2^\circ\end{aligned}\quad (11)$$

For typical real cases, we will have efficient diffraction only in situations where the light wave's direction of propagation is nearly normal to that of the sound wave.

Extending to Traveling Waves

Up to now we have considered only standing acoustic waves. Extending the analysis to traveling acoustic waves presents no problem. Since the speed of the sound waves is much less than that of the light waves, the traveling wavefronts — to a good approximation — do not move during the time in which they interact with individual light waves. Thus, we can effectively regard all cases as the standing-wave case.

A traveling acoustic wavefront will produce one effect on an incident light beam worth noting — a Doppler shift. The frequency shift may be either positive (light frequency increased) or negative (light frequency decreased), depending on

whether the light wave annihilates or creates an acoustic phonon in the interaction. Measurements of these shifts are referred to as Brillouin spectroscopy. The shifts are of the order of the phonon frequency, typically 1 GHz or less, and are thus small and difficult to measure. For most applications of acousto-optic devices, this shift can be safely ignored.

In any real case, both reflected

and refracted light waves will be present. While this discussion — particularly the analogy of the stack of glass plates — centers around the reflected wave, the refracted wave is also useful. Remember that the refractive index modulations produced by the sound waves are not perfectly reflecting; the remainder of the light wave is refracted, just as in the case of a glass plate.

A basic physical problem confounds the designer wishing to use standing acoustic waves in an acousto-optic device. Standing waves exist only when the acoustic frequency and medium dimensions allow an integral number of half-wavelengths of the acoustic wave to fit precisely within the medium boundaries. This would require precise control of acoustic frequency and medium dimensions, including precise temperature stabilization. Thus, it is not surprising that most acousto-optic devices utilize traveling acoustic waves. For traveling acoustic waves, the designer's primary concern is interference effects resulting from reflections at the medium boundaries. These can be eliminated by proper design with modest effort.

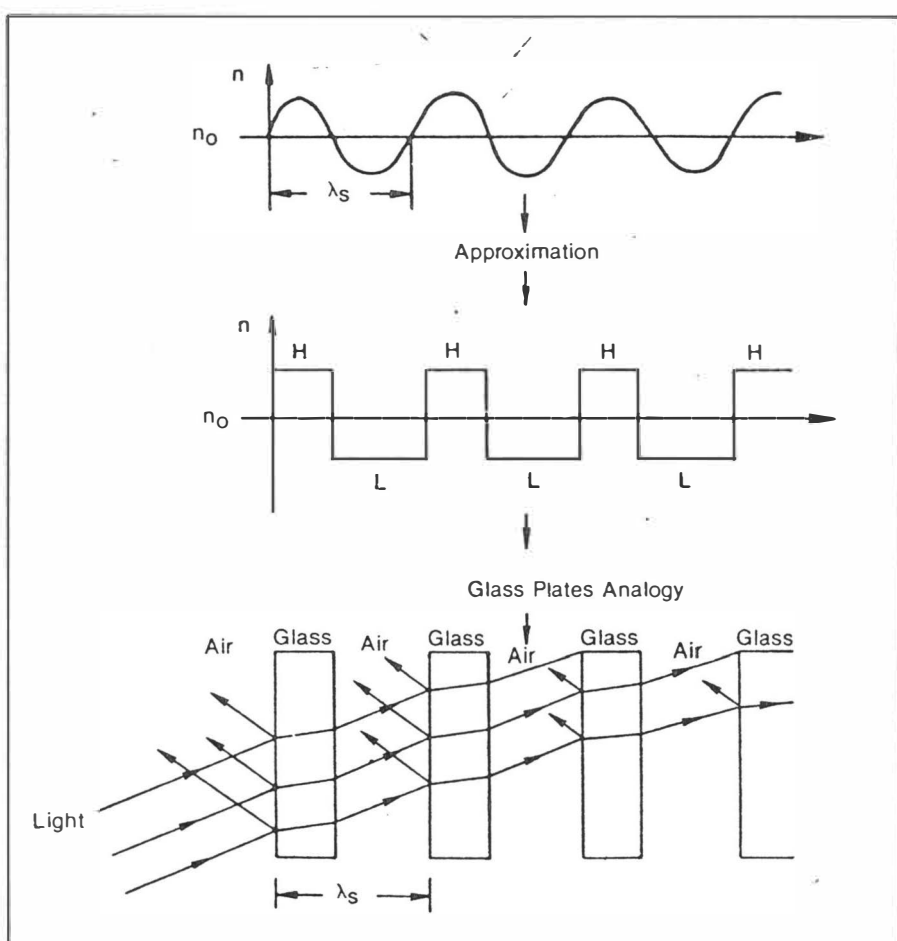


Figure 4. The periodic variations in refractive index noted in Figure 3 can be approximated by a stack of glass plates that give rise to periodic reflections and refractions.

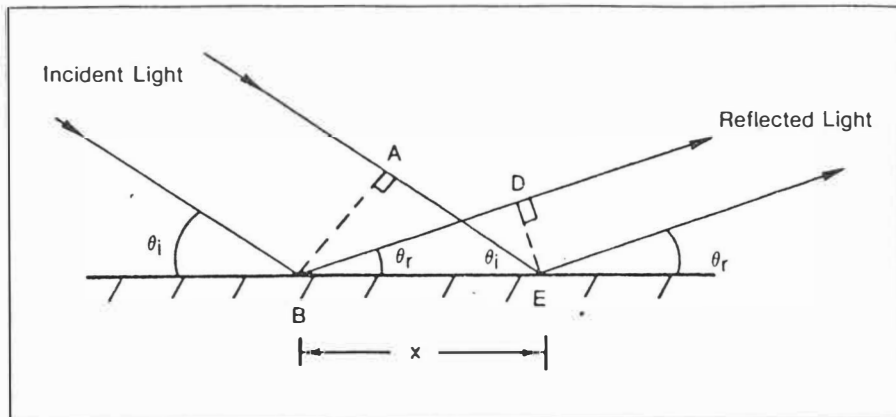


Figure 5. Geometry of reflection at a single interface (per the analogy of the stack of glass plates in Figure 4).

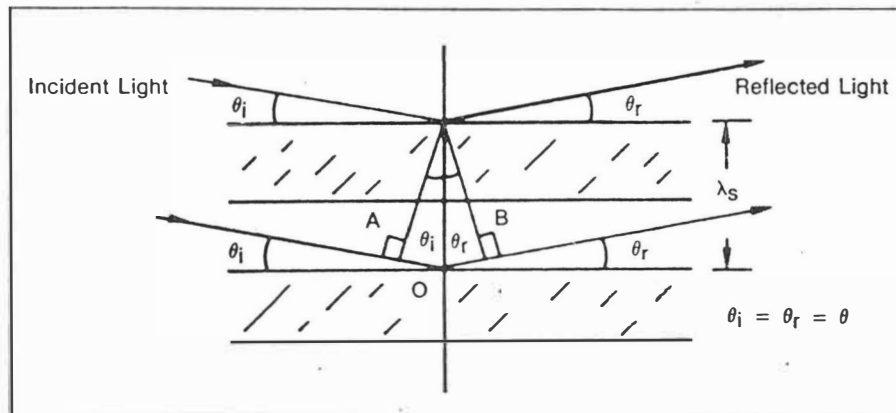


Figure 6. Geometry of reflection at two adjacent interfaces (per the analogy of the stack of glass plates in Figure 4).

Diffraction Efficiency

One of the most useful parameters for determining performance of an acousto-optic device is the diffraction efficiency. It is the fraction of the incident light beam diffracted into a specific diffracted beam. Some involved derivation yields the following formula for diffraction efficiency

$$E = \frac{I_d}{I_i} \quad (12)$$

$$= \sin^2 \left\{ \frac{\pi l}{2^{1/2} \lambda_i} \left[\frac{n_0^6 p^2}{\rho_0 C_s^3} I_{ac}^{1/2} \right] \right\}$$

Here, ρ is the diffraction efficiency, l is the interaction length (approximately equal to the optical path of the light beam in the acoustic beam), n_0 is the index of refraction of the medium at the wavelength of interest (in the quiescent state), p is the photoelastic constant of the material, ρ_0 is the mass density of the material, λ_i is the incident light wavelength in the material ($= \lambda_0/n_0$, where λ_0 is the vacuum wavelength of the incident light), and I_{ac} is the input acoustic intensity to the device (measured in watts per meter squared).

Acoustic Frequency

Another parameter of importance is the acoustic frequency. We need very high acoustic frequencies to produce any observable effects. Why? The angular separation between diffracted orders (the angle between light beams that interact

with zero, one, two, etc. acoustic wavefronts) is approximately

$$|\Theta_{d1} - \Theta_{d2}| = \Delta \Theta_d \equiv \frac{\lambda}{\lambda_s} = \frac{v_s}{v} \quad (13)$$

Clearly, this ratio must be large if we are to have good separation of the orders and large diffraction angles. For the first-order diffracted beam to be separated from the zeroth-order (undiffracted) beam by 1° (1.7×10^{-2} radians) at 514.5 nm (5.8×10^{14} Hz), we need $v_s = 10^{11}$ Hz.

Product literature frequently refers to two acoustic frequencies. One is the carrier frequency, the frequency of the input acoustic power. The second is the modulation frequency, the frequency with which we modulate the input acoustic power. This modulation frequency is typically much less than the carrier frequency.

In most acousto-optic devices, $\Delta \theta_d$ ranges from 10^{-4} to 10^{-2} to produce measurable effects. This value should be large for a beam deflector, but it can be much smaller for a modelocker, where beam deflection is not the primary objective of the device.

Device Characteristics

All the devices to be described here are basically the same. The major differences arise from the manner in which they are used. Commercial devices are optimized for particular applications, so users shouldn't expect to achieve good results by trying to perform beam deflection, for example, with a modelocker that happens to be at hand.

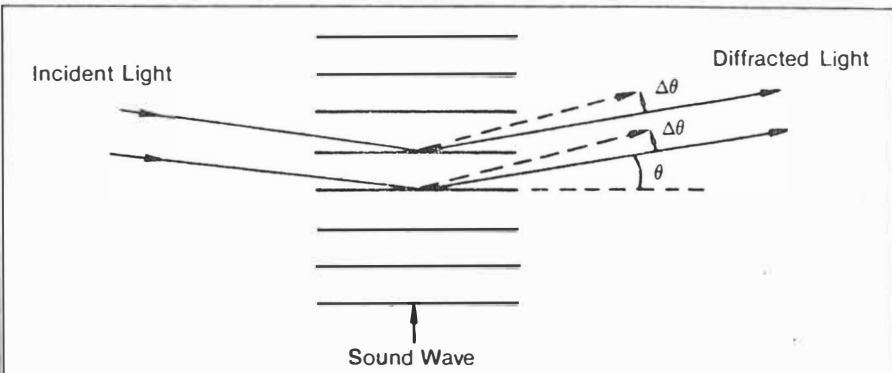


Figure 7. Beam deflection near the Bragg condition, as is typical of a beam deflector used as a cavity dumper.

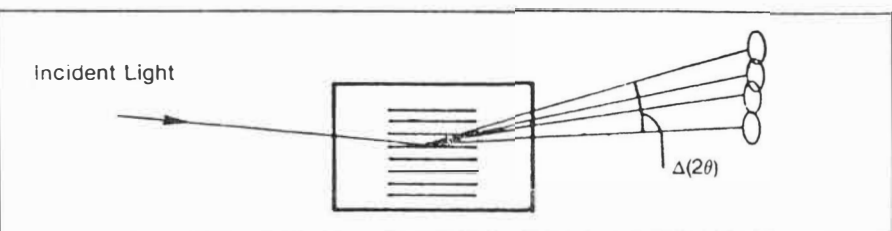


Figure 8. Beam deflection produces a nominal number of resolvable spots.

In order to keep the discussions of the devices simple, many details of device construction will be ignored. Although these details optimize device performance, they don't

necessarily enhance understanding of the device's basic operation. In particular, we'll not consider any reflections at device interfaces, nor will we calculate the refraction that

occurs as the light leaves the device. Since this refraction would normally increase the deflection angles, angles calculated here will be smaller than those encountered with actual devices. We also consider only first-order diffraction, neglecting higher orders.

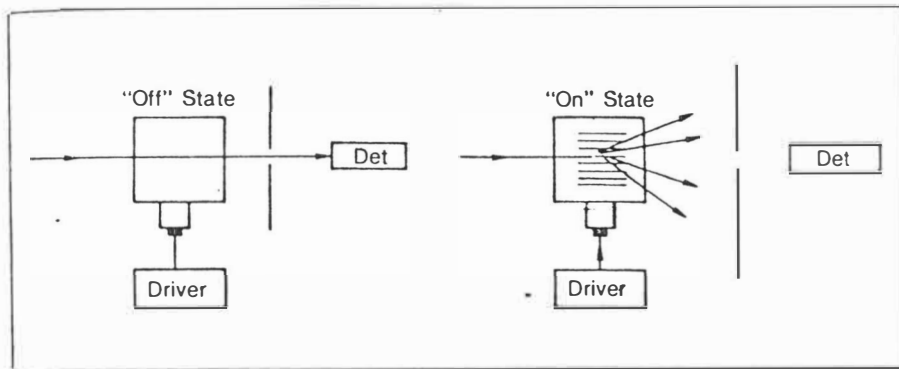


Figure 9. Beam modulation over "on" and "off" states.

Table 2 — Types of Acousto-Optic Devices

Type of Cell	Characteristics
Diffraction Cell	This device merely diffracts an input beam. The characteristics of the output beams are not relevant except in the cases of imaging devices. Examples include modelockers and simple modulators.
Beam Modulator	This device turns an input beam "on" and "off" with possible intermediate states, but it maintains beam quality under all conditions down to the "off" state. The primary example would be an RF communications device.
Beam Deflector	This device deflects an input beam through a (possibly variable) angle $\Delta(2\theta)$ in a controllable fashion. Beam characteristics and quality are maintained under all conditions. Examples include deflectors for laser writing applications and cavity dumpers.
Phase Modulator	This device shifts the phase of an input beam by an amount, possibly variable, in the "on" state. One example is an acousto-optic delay line.
Focuser/Defocuser	This device focuses or defocuses a beam while maintaining other beam characteristics. In effect, this device uses cylindrical acoustic waves as a lens.
Frequency Shifter	This device shifts the frequency of an input light beam up or down while maintaining other beam characteristics. Examples include an optical spectrum analyzer and devices for producing beat frequencies for optical information processing.
Image Projector	Such a device will "break up" or transmit without distortion in a controllable fashion. As such, it can deflect or project an optical image. An example would be in the projection of large-screen television images.
Information Processor	Here, a variable phase grating generated by acoustic wave in a transparent medium replicates an input very-high-frequency signal. This is used to spatially modulate a light beam. Thus, an input electrical signal can be processed by spatial correlation techniques applied to a light beam transmitted through the medium.
Convert Light Into Sound	This can happen in two related ways and is the inverse of the Debye-Sears effect. In one case, high-energy light beams create sound waves in a transparent material at their difference (beat) frequency. In other cases, pulsed high-energy light beams generate sound in a material at the pulse frequency — thermally produced sound. The sound originates from thermal expansions or contractions of the material resulting from deposition of beam energy in the material.

Cavity Dumper

We can deflect a light beam acousto-optically by changing the sound frequency, ν_s , while operating near the Bragg condition (Figure 7). Recall the Bragg condition:

$$2 \lambda_s \sin \Theta = 2 \frac{c_s}{\nu_s} \sin \Theta = \lambda \quad (14)$$

For constant λ and c_s , a change in ν_s of $\Delta\nu_s$ gives (taking advantage of the small-angle approximation)

$$\Delta(2\Theta) \cong \left(\frac{\lambda}{c_s} \right) \Delta \nu_s \quad (15)$$

Thus, by changing the carrier frequency at some lower modulation frequency, we can deflect the beam through an angle proportional to the change in the carrier frequency at a deflection frequency equal to the modulation frequency. For SiO_2 with $\lambda = 600 \text{ nm}$ and $\Delta\nu_s = 400 \text{ MHz}$, $\Delta(2\Theta) = 0.04^\circ$ radians, or about 2° . Here, changing the carrier frequency from 100 MHz to 500 MHz ($\Delta\nu_s = 400 \text{ MHz}$) at a modulation frequency of 1 MHz, we can deflect a 600-nm light beam through an angle of about 2° from its original direction at a deflection frequency of 1 MHz.

Beam Deflector

The important performance parameter of an acousto-optic beam deflector is not the deflection angle, but the number of resolvable "spots" (discrete, resolved beams) it can project on a screen at an arbitrary distance from the device. We define this parameter as the number of spots, N . N is the factor by which $\Delta(2\Theta)$ exceeds the divergence angle of the diffracted beam for a given set of operating conditions.

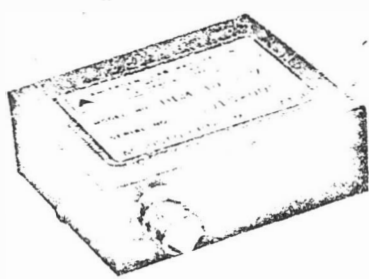
The beam divergence angle is approximately the diffraction limit, λ/D , where D is the diameter of the diffracted beam. According to our definition, if we let the beam divergence angle be $\theta_{\text{div}} = \lambda/D$, then

$$N = \frac{\Delta(2\Theta)}{\theta_{\text{div}}} = \left(\frac{\lambda}{c_s} \right) \frac{\Delta \nu_s}{\lambda/D} = \Delta \nu_s \left(\frac{D}{c_s} \right) = \Delta \nu_s \tau \quad (16)$$

ACOUSTO-OPTIC MODULATORS

For over 15 years, Andersen Laboratories has been in the forefront of controlling and switching laser power. Our field proven modulators feature the following:

- Operating wavelengths 300-1150 nanometers
- Modulation bandwidths up to 14 MHz @ -3dB
- Deflection efficiencies greater than 85%
- Drivers available



OTHER QUALITY OPTICAL COMPONENTS

- Q-Switches
- Beam Deflectors
- Mode Lockers

 ANDERSEN LABORATORIES
1280 Blue Hills Avenue
Bloomfield, CT 06002
TEL (203) 242-0761
TWX 710-425-2390

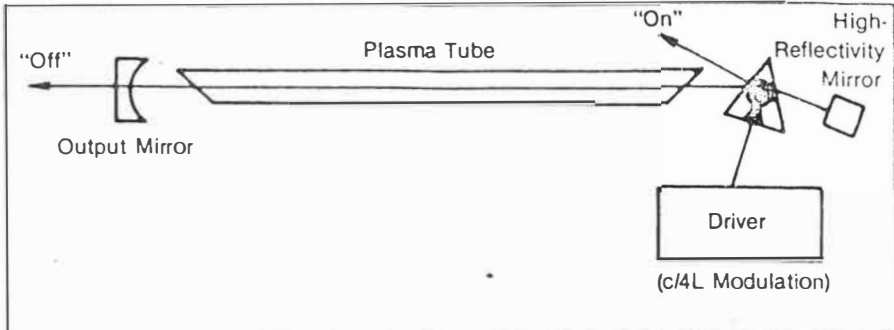


Figure 10. Modelocking involves switching the beam out of the active lasing medium at a rate of $c/4L$.

where τ is the time required for sound to cross the light beam's diameter. Referring to Figure 8, and using our previous example of SiO_2 , $\lambda = 600 \text{ nm}$, and $\Delta\nu_s = 400 \text{ MHz}$, Equation 16 yields a value of N of approximately 66 resolvable spots.

In an information system, if we use a linear detector array, then N is the number of information channels we can address independently. Optimized commercial acousto-optic beam deflectors can reach values of $N = 1,000$. This value makes such applications areas as information processing and laser writing/graphics potentially quite appealing.

Beam Modulator

In a simple case (Figure 9), in the quiescent state, incident light travels through the crystal into the aperture and strikes the detector. When acoustic power drives the crystal, the beam is diffracted away from the aperture and is not detected.

A beam deflector can be used as a modulator merely by the addition of a mask at the beam exit. By controlling the change in the acoustic power frequency, we can cause the exiting beam to pass through the mask or be blocked by it.

In principle, an acousto-optic beam modulator is precisely the same as an acousto-optic beam deflector but is used in a different mode. In commercial devices, however, a modulator will generally be optimized so that it has the highest possible frequency response for a minimum input frequency change, high extinction ratio, and low losses. A deflector will be optimized to have large deflection angle and a large N .

Modelocker

The modelocker depicted in Figure 10 can be viewed in several ways.

First, it is an acousto-optic modulator, where the aperture of Figure 9 is the plasma tube's bore.

In the quiescent state the beam passes through the prism and into the bore. When acoustic power is applied, the beam is deflected to miss the bore. Lasing is interrupted until the acoustic power again reaches zero. If the acoustic power is modulated at a frequency of $c/4L$, where L is the optical length of the cavity, the acoustic power will pass through zero twice during a round-trip cavity period, and phase locking of the cavity modes will take place.

Second, it is an acousto-optic beam deflector. The description is the same as in the preceding paragraph.

Third, it is an acousto-optic diffraction cell. When acousto-optic power is present in the prism, the beam is diffracted, at least in part, away from its intended path through the plasma tube's bore. The intracavity power is reduced to the point where round-trip gain falls below lasing threshold. When the acoustic power is "off," there is no attenuation of the intracavity power, and the laser resumes lasing in the free-running mode. If the acoustic power is turned "on" and "off" at frequency $c/4L$, phase locking of the cavity modes will occur.

Commercial modelockers are optimized for high performance at modulation frequency $c/4L$, low losses in the "off" condition, large losses in the "on" condition, and sharp transitions between the two states.

Table 2 summarizes the various types of acousto-optic devices. □

References

1. A. Yariv, *Introduction to Optical Electronics*, Chapter 12, pp. 305-321.
2. R. Adler, "Interaction Between Light and Sound," *IEEE Spectrum*, May 1967, pp. 42-54.
3. D. Maydan, "Acousto-optical Pulse Modulators," *IEEE J. of Quant Elec.*, **QE-6**:15-24, January 1970.
4. D. Maydan, "Fast Modulator for Extraction of Internal Laser Power," *J. of Appl. Phys.*, **41**:1552-1553, March 1970.

Experiments on the Interaction of Light and Sound for the Advanced Laboratory

D. T. PIERCE*

R. L. BYER

Applied Physics Department

Stanford University

Stanford, California 94305

(Received 12 June 1972; revised 10 October 1972)

We describe an advanced laboratory experiment in which both Raman-Nath and Bragg diffraction of light by acoustic waves in water are observed in the sound frequency range from 5 to 45 MHz. The apparatus consists of a laser, light detector, rf power source, quartz transducer, and homemade water cell. We discuss the theory of Raman-Nath diffraction, Bragg diffraction, and the criteria for the manifestation of each. The measured Raman-Nath diffracted orders give a visual display of FM sidebands. We discuss a quantitative relationship between the incident and diffracted light and the sound for Bragg diffraction in terms of a three-wave parametric process. Stanford students in the Advanced Applied Physics Laboratory have successfully performed this experiment during the past three years.

cell. This experiment has been well received in a graduate laboratory taught at Stanford which draws students from physics, applied physics, and electrical engineering. We believe that this experiment would also be suitable for a senior laboratory.

In 1922 Brillouin¹ presented a theory of light scattering from thermally excited elastic waves. He predicted that light would be diffracted by elastic waves in solids and liquids at the Bragg angle α given by $\sin\alpha = \lambda/2\Lambda$, where λ and Λ are the wavelengths of light and sound in the medium. The diffuse scattering of x rays has been extensively studied to determine thermal phonon distributions and the elastic constants of crystals.²⁻³ In 1932 Debye and Sears⁴ in the United States and, independently, Lucas and Biquard⁵ in France first observed the diffraction of light by artificially generated elastic waves. These early experiments showed diffraction into several higher orders and a distribution of intensity in the higher orders that could not be explained by ordinary Bragg diffraction. A few years later Raman and Nath⁶⁻¹⁰ in a series of papers developed a theory which explained the experimental observations.¹¹

The interaction of light and sound displays different characteristics depending on the width of the interaction region, the light and sound wavelengths, and the amplitude of the sound wave. Roughly speaking, if the width, frequency, and amplitude of the sound beam are sufficiently small, the observed diffraction is explained by the theory of Raman and Nath and frequently is referred to as Raman-Nath diffraction. Conversely, Bragg diffraction is observed if the width, frequency, and amplitude of the sound beam are sufficiently large. We discuss quantitative criteria for these two types of diffraction in Sec. II. In Sec. II.A we discuss the Raman-Nath theory, which shows that the acoustic beam can be treated as a phase grating which modulates the light similar to FM wave modulation. A powerful approach to the interaction of light and sound in the Bragg regime is to treat it as a three-wave

I. INTRODUCTION

The interaction of light and sound exhibits many interesting and useful effects. Sound waves can deflect light, change its frequency, and modulate its phase and amplitude. In turn the diffracted light can probe the spatial distribution of acoustic energy in the sound beam and give information on the velocity and attenuation of the sound wave and the elastic properties of the material.

All of these phenomena are dramatically observed in the laboratory experiment we describe here. A minimum of equipment is required: a HeNe laser, an rf power source, a light detector, a quartz crystal transducer, and a homemade water

parametric process.¹² Our discussion of this approach to Bragg diffraction in Sec. II.B is of interest since other phenomena such as optical parametric oscillation, Brillouin scattering, and Raman scattering can be treated analogously. The Bragg angle condition and the frequency shift of the light results naturally from conservation of energy and momentum when treated as a parametric process.

In this experiment we explore the diffraction of light from traveling waves in a liquid over the wide range from Raman-Nath to Bragg diffraction. The somewhat related recent article by Kang and Young¹³ discusses Raman-Nath diffraction from standing waves with particular emphasis on determining the length of the sound wave and understanding the physical optics behind the striation pattern observed in the Schlieren method.

In Sec. III we discuss the apparatus used in our laboratory experiment and the observed Raman-Nath and Bragg diffraction results. The ultrasonic wave is conveniently generated in water which diffracts light very efficiently. The full range of Raman-Nath and Bragg diffraction is observed in the acoustical frequency range of 5 to 45 MHz. The use of a HeNe laser with its monochromatic, well collimated beam greatly facilitates the experiment.

The development of the laser and improvements in acoustical techniques, particularly in the microwave region, have generated renewed interest in the interaction of light and sound and have rendered feasible new applications and the observation of new phenomena. Many of the applications rest directly on the basic experimental results of Sec. III while others require some extensions of these experiments.

II. THEORY

A. Raman-Nath Diffraction

Figure 1 shows the essentials of the Raman-Nath diffraction where a light wave with wave vector \mathbf{k} , frequency ω , and wavelength λ in the medium is incident parallel to the wavefronts of a traveling sound wave characterized by \mathbf{k}_s , ω_s , and wavelength Λ . At any instant in time the sound wave creates alternate regions of compression and expansion, periodic variations in density

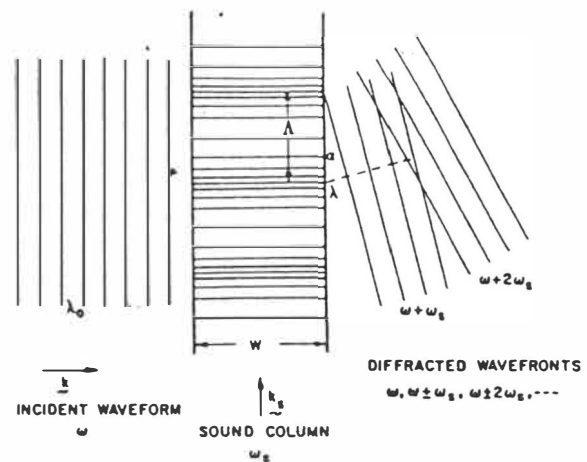


FIG. 1. Schematic drawing of Raman-Nath diffraction. Light incident on the sound column of width W , frequency ω_s , and wavelength Λ is diffracted at frequencies $\omega \pm \omega_s$, $\omega \pm 2\omega_s$, etc., and approximate angles λ/Λ , $2\lambda/\Lambda$, etc.

which produce a periodic variation in the refractive index. To introduce the Raman-Nath theory we assume that the width W of the sound wave is small enough so that curvature of the light rays is negligible. Only the velocity and therefore the phase of the light changes with the variation of the refractive index. The light wave emerges from the sound wave with its amplitude constant but its phase a periodic function of position with a period Λ . Hence the sound wave acts like a phase grating. The change in phase $\Delta\phi$ of a light wave passing through a region where the normal refractive index n is changed by Δn is given by

$$\begin{aligned}\Delta\phi &= W\Delta k = W(\omega/c)(n + \Delta n) - (W\omega n/c) \\ &= 2\pi W\Delta n/\lambda_0,\end{aligned}\quad (1)$$

where λ_0 is the light wavelength in a vacuum. The change in the refractive index is related to the change in density by $\Delta n/n = \Delta\rho/\rho$. The sound power density P_s is given by¹⁴

$$P_s = \rho \frac{1}{2} v^3 (\Delta\rho/\rho)^2 = \frac{1}{2} (\rho v^3) (\Delta n/n)^2. \quad (2)$$

The light emerging from the sound wave interferes destructively except along certain directions. To find the direction of the diffracted light we return to Fig. 1 and construct wavefronts connecting points of the same phase. The light deflects into higher orders on each side of the

undeflected beam at an angle α for the q th order given by

$$\sin\alpha = \pm q(\lambda/\Lambda). \quad (3)$$

In practice α is very small so that $\alpha \approx \pm q(\lambda/\Lambda)$. For angles measured in air instead of in the medium in which the sound wave is generated, $\alpha \approx \pm q(\lambda_0/\Lambda)$ when the optical boundary of the medium is parallel to the sound beam.

The periodic variation of the phase of a wave is familiar in another context, namely FM systems. The sinusoidally varying index of refraction phase modulates the light wave at a frequency ω_s , with the phase excursion or modulation index of $\Delta\phi$ given by Eq. (1). The carrier corresponds to the zero-order (undiffracted) light wave and the side bands at $\omega \pm \omega_s$, $\omega \pm 2\omega_s$, ... to the higher order diffracted light waves. The amplitude of the phase modulated light wave is

$$\begin{aligned} E &= E_0 \exp(-i\omega t + i\Delta\phi \sin\omega_s t) \\ &= E_0 \exp(-i\omega t) \sum_{q=-\infty}^{\infty} J_q(\Delta\phi) \exp(iq\omega_s t), \end{aligned} \quad (4)$$

where we have expanded in terms of ordinary Bessel functions $J_q(\Delta\phi)$.¹⁵ Each higher order at frequency $\omega \pm q\omega_s$ has an intensity proportional to $J_q^2(\Delta\phi)$. The corresponding orders on each side of the undiffracted beam have equal intensity since $J_q^2(\Delta\phi) = J_{-q}^2(\Delta\phi)$. Figure 2 shows the relative intensity of light $J_q^2(\Delta\phi)$ in the first four orders. Notice that a traveling acoustic wave diffracts all of the light out of the zeroth order when $\Delta\phi = 2.4$ rad. Because of the sum rule,

$$J_0^2(\Delta\phi) + 2 \sum_{q=1}^{\infty} J_q^2(\Delta\phi) = 1, \quad (5)$$

light diffracted out of one order must appear in another.¹⁶

So far we have considered light incident parallel to the acoustic wavefronts. In one of their later papers Raman and Nath⁷ calculated the case of light incident obliquely at an angle θ to the acoustic wavefront. Then the intensity in order q was shown to be given by

$$I_q \propto J_q^2 \left(\Delta\phi \sec\theta \frac{\sin(\pi W \tan\theta/\Lambda)}{\pi W \tan\theta/\Lambda} \right). \quad (6)$$

The diffraction pattern is symmetric at all angles of incidence, that is, $I_q = I_{-q}$ for all θ . Note also that the intensity of each order as a function of angle of incidence is symmetric about normal incidence, $\theta = 0$.

As mentioned previously, the above discussion applies to progressive ultrasonic waves. If the wave is reflected and standing waves are established, the situation is quite different. Twice each period the amplitude of the standing wave is zero everywhere and the ultrasonic grating is canceled. At these times all of the light is undiffracted and falls in the zero order so that it is never possible to completely eliminate the zero-order light. The total amount of light diffracted into higher orders is correspondingly smaller. The entire diffraction pattern is modulated with a frequency $2\omega_s$. Each order of light diffracted from standing waves contains numerous frequency components. The zero order and each even order have frequency components at all even harmonics ω_s , $\omega_s \pm 2\omega_s$, $\omega_s \pm 4\omega_s$, etc., while each odd order has frequency

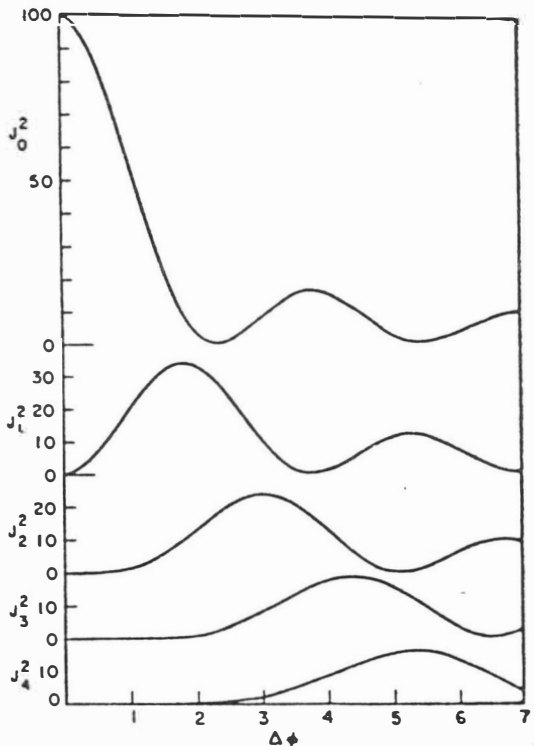


FIG. 2. The relative light intensity varies as $J_q^2(\Delta\phi)$ in the q th order for a phase change $\Delta\phi$ in the case of Raman-Nath diffraction from a progressive wave.

W = width of the sound wave.

components at all odd harmonics $\omega \pm \omega_0$, $\omega \pm 3\omega_0$, $\omega \pm 5\omega_0$, etc. The distribution of light intensity in the various orders is somewhat more complicated than in the case of diffraction from a progressive wave.⁸

The Raman-Nath theory described above is applicable when the curvature of the light beam towards regions of higher refractive index is negligible. The curvature can be negligible for several reasons: (1) The variation in refractive index Δn is so small as to cause little curvature; (2) the width of the sound beam W is short enough so the integrated bending as the light traverses the sound beam is very small; or (3) the sound wavelength Λ is so long that the light can be bent some distance without passing through a region of significantly different Δn and hence the phase mismatch due to bending between the entering and emerging light ray is small. It is useful to have some criteria that takes account of these parameters and indicates the range of applicability of the Raman-Nath theory.

Lucas and Biquard⁵ calculated the curvature of light rays incident from left to right and parallel to the acoustic wavefronts as shown in Fig. 3. The abscissa is the normalized distance into the sound beam $W' = 2\pi W(\Delta n/n)^{1/2}/\Lambda$. The light rays converge and first cross at $W' \approx \pi/2$. For W' near to and larger than $\pi/2$ the intensity distribution of the emerging light varies periodically along the sound beam with period Λ . Thus the sound wave acts as both a phase and an amplitude grating and the intensity in the diffracted orders is not

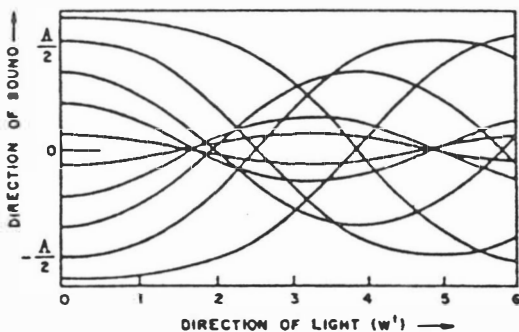


FIG. 3. Light incident from the left parallel to the acoustic wavefronts is bent toward regions of higher refractive index. The width of the sound column must be such that $W' < \pi/2$ from Raman-Nath diffraction (after Lucas and Biquard, Ref. 5).

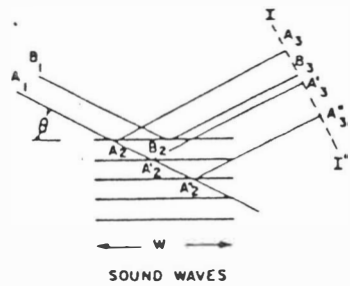


FIG. 4. For Bragg diffraction the incident and diffracted angles are equal, the pathlengths must be equal which requires $m\lambda = 2\Lambda \sin\theta$, and the sound column must be wide enough so that the light crosses at least two wavefronts.

~~Eq. (4) = plane wave.~~

given by Eq. (4). The amplitude grating effect becomes smaller as W' decreases below $\pi/2$. Willard¹⁴ determined experimentally that diffraction measurements agree with the Raman-Nath theory within 10% when $W' \leq \pi/2$. Thus the relation between W , Λ , and Δn for Raman-Nath diffraction is

$$W \leq \frac{1}{4} \Lambda (n/\Delta n)^{1/2}$$

or

$$W \leq (\Lambda^2/16)(n/\lambda)(2\pi/\Delta\phi). \quad (7)$$

The criterion is somewhat arbitrary since there is no distinct line where suddenly the Raman-Nath theory becomes appropriate. Another criterion frequently used¹⁵ ignores the sound intensity and considers only the phase mismatch caused by the diffraction of the light through the equivalent aperture $\Lambda/2$. The phase mismatch of the entering and emerging light due to the diffraction of the aperture is $4\pi W\lambda/\Lambda^2$. For the mismatch to be less than $\pi/4$ we have

$$W \leq \Lambda^2/16\lambda, \quad (8)$$

which is approximately equivalent to the previous criterion as long as $\Delta\phi < 2\pi$.

Both the amplitude and phase changes of the light are accounted for by a partial differential equation describing light propagation in a medium with sound waves. Raman and Nath obtained a set of coupled differential-difference equations that describe the general case. In the Raman-Nath region where Eq. (7) holds, the approximate

solution to these equations shows that the diffracted light has the expected Bessel function amplitudes. In the region where both amplitude grating and phase grating effects are important the general differential-difference equations no longer have simple analytic solutions. They have been solved numerically using a computer by Klein and Cook¹⁷ to show the nature of the diffracted light in the transition region from Raman-Nath diffraction to Bragg diffraction.

B. Bragg Diffraction

When the sound beam is wide and the sound wavelength short, the diffracted light is a maximum when it is incident on the sound wave front at a particular angle. Also the diffracted light is in a single order on one side of the undiffracted beam. Figure 4 illustrates the physical reasons for this behavior.¹⁴ Consider light rays $A_1A_2A_3$ and $B_1B_2B_3$ scattered from two points A_2 and B_2 on a given sound wave front. The light is in phase and interferes constructively at the plane II' perpendicular to the reflected rays if the path lengths $A_1A_2A_3$ and $B_1B_2B_3$ are equal. The path lengths are equal if the incident and reflected angles are equal. Only some of the light scatters at the first wavefront. That light which scatters at equal angles from subsequent wavefronts at A_2' and A_2'' in Fig. 4 is in phase with light scattered at A_2 if the path lengths differ by an integral number of light wavelengths. Such constructive interference takes place at certain angles given by the Bragg relation

$$m\lambda = 2\Lambda \sin\theta. \quad (9)$$

The reinforcement from scattering at successive sound wavefronts, which is a criteria for Bragg diffraction, only occurs if the incident light ray passes through at least one entire sound wavelength. The more sound wavefronts N which the light ray crosses, the sharper and more intense is the diffracted light. Since the angles are small, we use the relation $\sin\theta = m\lambda/2\Lambda$ from the Bragg equation and $W \tan\theta = N\Lambda$ from Fig. 4 to give a minimum criteria for Bragg diffraction in the order m ¹⁸

$$W \geq 2N\Lambda^2/m\lambda, \quad (10)$$

where $N \geq 1$. Here we refer to angles inside the medium with index of refraction n . The same

Bragg condition holds if both the angle and light wavelength are measured in air. While no dependence on sound amplitude appears in the criteria of Eq. (10), Klein and Cook¹⁷ have pointed out that true Bragg reflection also requires $\Delta\phi \ll 2\pi\lambda W/\Lambda^2 n$.

The frequency of the diffracted light ω_2 is Doppler shifted from the incident light frequency ω_1 by an amount equal to the sound frequency ω_s . The light diffracted from the oncoming sound waves toward the direction of sound propagation has an increased frequency while the light diffracted in the opposite direction from receding sound waves has a lower frequency. The Doppler shifted frequency ω_2 of the light diffracted through the angle 2θ from its initial direction is given by

$$\omega_2 = \omega_1 [1 \pm 2(nv/c) \sin\theta], \quad (11)$$

and since $\sin\theta = m\lambda/2\Lambda$, we have $\omega_2 = \omega_1 \pm \omega_s$.

The diffraction process can be viewed in terms of quantized light and sound whereby an incoming photon collides with a phonon suffering a change in momentum and energy as illustrated by the

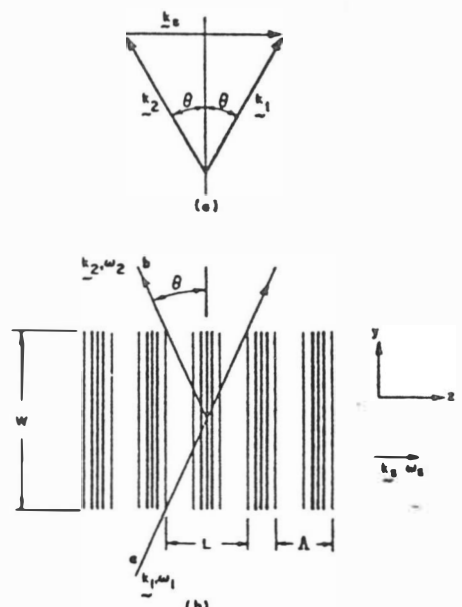


FIG. 5. (a) Momentum conservation diagram. (b) The Bragg diffraction configuration discussed in the calculation. The incident wave labeled a is at frequency ω_1 and the diffracted wave b is at $\omega_2 = \omega_1 - \omega_s$. The length of the interaction region is $L = W \tan\theta$.

vector diagram in Fig. 5(a). The conservation of energy and momentum provides the following relations:

$$\omega_1 = \omega_2 + \omega_s \quad (12)$$

and

$$\mathbf{k}_1 = \mathbf{k}_2 + \mathbf{k}_s, \quad (13)$$

which is equivalent to saying the frequency is Doppler shifted.

A powerful quantitative approach to this problem is to treat Bragg diffraction as a three-wave parametric interaction. We present this approach briefly following Quate *et al.*¹² The sound input ω_s interacts with the pump at ω_1 to produce the signal at $\omega_2 = \omega_1 + \omega_s$. Consider Fig. 5(b) where we show light waves with fields E_a (at ω_1) and E_b (at ω_2) both polarized in the x direction. The total field $E_z = E_a + E_b$ satisfies the wave equation

$$(\partial^2 E_z / \partial y^2) + (\partial^2 E_z / \partial z^2) = \mu (\partial^2 D_z / \partial t^2). \quad (14)$$

In the absence of sound the electric fields propagate as plane waves

$$\begin{aligned} E_a &= \frac{1}{2} E_1 \exp[i(\omega_1 t - k_1 z \sin\theta - k_1 y \cos\theta)] + \text{c.c.} \\ &= \frac{1}{2} E_1 \exp(i\phi_1) + \text{c.c.} \end{aligned} \quad (15)$$

and

$$\begin{aligned} E_b &= \frac{1}{2} E_2 \exp[i(\omega_2 t + k_2 z \sin\theta - k_2 y \cos\theta)] + \text{c.c.} \\ &= \frac{1}{2} E_2 \exp(i\phi_2) + \text{c.c.} \end{aligned} \quad (16)$$

The interaction takes place because the index of refraction of the medium is modulated by the change in density produced by the acoustic wave through the photoelastic effect. We assume that the intensity of the sound wave is unchanged by the interaction. For an acoustic wave giving rise to a periodic strain

$$S = \frac{1}{2} S \exp[i(\omega_s t - k_s z)] + \text{c.c.} = \frac{1}{2} S \exp[i\phi_s] + \text{c.c.}, \quad (17)$$

the change in the dielectric constant is given by

$$\Delta\epsilon/\epsilon = (-\epsilon/\epsilon_0) p S, \quad (18)$$

where p is the elasto-optical coefficient. In the case of a crystal p is a fourth-rank tensor relating different directions of strain and optical polarization.¹⁸ Therefore, we have for the displacement

$$D = (\epsilon + \Delta\epsilon)(E_a + E_b). \quad (19)$$

Substituting the electric fields and strain wave into the wave equation one obtains a coupled set of equations

$$dE_1/dz = (ik_1 n^2 p / \sin\theta) (S/2) (E_2/2), \quad (20)$$

$$dE_2/dz = -(ik_2 n^2 p / \sin\theta) (S/2) (E_1/2). \quad (21)$$

In deriving these equations (which include their complex conjugates), we have assumed that E_1 and E_2 are slowly varying in the z direction so that d^2E/dz^2 is negligible. In addition, for cumulative interaction the frequency and wave vector of the source and driven terms must be the same. This requires $\phi_1 = \phi_2 + \phi_s$ which leads to the conservation conditions

$$\begin{aligned} \omega_1 &= \omega_2 + \omega_s, \\ k_1 \sin\theta + k_2 \sin\theta &= k_s, \\ k_1 \cos\theta &= k_2 \cos\theta. \end{aligned} \quad (22)$$

The amplitudes E_1 and E_2 of the waves vary in the z direction as $\exp(\pm\Gamma z)$ where

$$\Gamma = k_1 \left(\frac{\omega_2}{\omega_1} \right)^{1/2} \frac{\epsilon}{2\epsilon_0} \frac{p}{\sin\theta} \left(\frac{P_s}{2\rho v^3} \right)^{1/2}, \quad (23)$$

and $P_s = \frac{1}{2} \rho v^3 S^* S$ is the power density of the sound wave. The length of the interaction region is $L = W \tan\theta$. With the boundary conditions $E_2(L) = 0$ and $E_1(0) = E_1$, we find

$$E_1 = E_1(0) [\cosh\Gamma(z-L)/\cosh\Gamma L] \quad (24)$$

and

$$E_2 = -E_1(0) \left(\frac{\omega_1}{\omega_2} \right)^{1/2} \left(\frac{S^*}{S} \right)^{1/2} \frac{\sinh\Gamma(z-L)}{\cosh\Gamma L}. \quad (25)$$

The ratio of the diffracted power to the incident power is

$$P_2/P_1 = |E_2(0)/E_1(0)|^2 = (\omega_2/\omega_1) \tanh^2 \Gamma L. \quad (26)$$

C.C. ≡ complex conjugate.

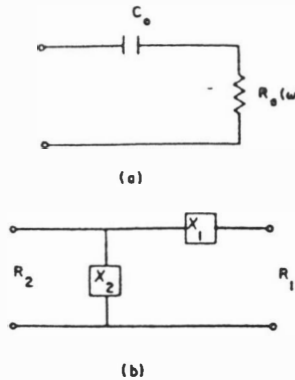


FIG. 6. (a) Electrical representation of the quartz crystal transducer. (b) L matching network.

For small ΓL , $\omega_1 \approx \omega_2$, and small θ this is approximately

$$P_2/P_1 = \frac{1}{2}\pi^2(n^6 p^2/\rho v^3)(W^2 P_s/\lambda_0^2), \quad (27)$$

where the material parameters have been grouped in the parentheses. For sound waves in water $\rho = 1$, $v = 1.5 \times 10^5$ cm/sec, $n = 1.33$, and from the Lorentz-Lorenz relation $p \approx 0.31$. Since v can be determined from the Bragg equation, it is possible to determine p from Eq. (27). For a crystal, of course, p would have different values depending on the crystal orientation. The elasto-optic coefficient p has been measured for a variety of materials.¹⁹⁻²¹

A special case of Bragg diffraction occurs for three waves propagating collinearly. At the correct sound frequency phase matching is guaranteed by the collinearity and a long interaction length can be obtained. In an anisotropic crystal Bragg scattering may lead to a change in polarization, a feature which has important practical applications as discussed in Sec. IV.